

**Influence of Saharan Aerosols on Phytoplankton Biomass
in the Tropical North Atlantic Ocean**

By
Aurora M. Justiniano Santos

A dissertation submitted partial fulfillment of the requirements for the degree of

DOCTOR IN PHILOSOPHY

in

Marine Sciences
(Biological Oceanography)

UNIVERSITY OF PUERTO RICO
MAYAGÜEZ CAMPUS
2010

Approved by:

Roy A. Armstrong, Ph.D.
Chairperson, Graduate Committee

Date

Yasmín Detrés, Ph.D.
Member, Graduate Committee

Date

José M. López, Ph.D.
Member, Graduate Committee

Date

Fernando Gilbes Santaella, Ph.D.
Member, Graduate Committee

Date

Ana Navarro, Ph.D.
Representative of Graduate Studies

Date

Nilda Aponte, Ph.D.
Chairperson of the Department

Date

Abstract

Atmospheric transport of aerosols from desert regions of Africa supply nutrients, such as iron, to oligotrophic oceanic waters. Phytoplanktonic organisms in surface waters use bio-available Fe, increasing their rate of photosynthesis. This work investigates the possible atmospheric Fe fertilization of oligotrophic North Atlantic and Caribbean waters. Level 3 weekly averaged images from SeaWiFS, MODIS Terra and MODIS Aqua satellite sensors were used to retrieve aerosol optical thickness (AOT) and chlorophyll concentration (Chl_a) data from Sept. 1997 through Dec. 2007. Results are presented for three areas in the Tropical North Atlantic Ocean and the Caribbean Sea, located at 17.5°N, 67.0°W, Caribbean Time Series Station (CaTS), 19°N, 57°W Western Atlantic Ocean and 20°N, 67°W Atlantic, North of Puerto Rico. A time series analysis exhibited a seasonal cycle with a summer maximum for mean AOT concentration. The strongest correlation between both parameters was observed for the Western Atlantic Ocean with a time-lag of approximately 1 month between AOT and Chl_a.

Visible reflectance spectroscopy (VRS) and trace element analysis were used to assess the presence of Fe in Saharan dust. Iron content was measured in samples from desert regions in Africa, starting from their source (African soil samples), their transformation across the Atlantic Ocean (Saharan dust collected at sea) and finally in the fraction reaching remote land areas (filtered air samples collected in Puerto Rico). Iron oxide mineral content was determined using reflectance spectroscopy and first derivative analysis. Distinctive peaks of two iron-bearing minerals, hematite and goethite, in the first derivatives were observed (555 to 580 nm for hematite and 435 nm for goethite). In addition, Fe and Al trace

element concentration was analyzed by inductively coupled plasma mass spectrometry (ICP-MS). The analysis showed evidence of the presence of Fe in all our samples. Results showed higher percent Fe in the finer particle size samples transported away from the desert.

Finally, satellite and *in-situ* AOT and Chl_a measurements were compared for the Tropical North Atlantic Ocean during March 2004 to observe the potential of satellite measurements in estimating atmospheric and oceanographic bio-optical properties. Aerosol and Chl_a measurements were obtained onboard the NOAA Ship Ronald H. Brown during the Aerosol and Oceanographic Science Expedition (AEROSE, February 29 - March 26 2004). This data were compared with two GIOVANNI (*GES DISC Interactive Online Visualization and ANalysis Infrastructure*) products, AOT (MODIS Aqua) and Assimilated Total Chlorophyll. Results showed a strong linear relation ($R^2 = 0.86$) between satellite and field AOT measurements. A strong relationship ($R^2 = 0.76$) was also observed between shipboard and satellite Chl_a, although the satellite product tended to underestimated chlorophyll concentrations relative to the field data. Also, monthly Giovanni's AOT and Chl_a products were compared to determine if a relationship between African dust input and Chl_a concentration can be established using Giovanni's satellite data. A time-lag of one month between AOT and Chl_a was also observed. Since the studied period (March 2004) coincided with one of the biggest dust storms for this season we examined AOT values and the North Atlantic Oscillation (NAO) index for the Western Atlantic Ocean Station (19°N, 57°W) to determine if the unusual dust event encounter during March 2004 was related to the NAO. A weak linear relationship between both parameters was observed.

Resumen

El transporte atmosférico de aerosoles desde regiones desérticas de África provee nutrientes, como hierro, hacia zonas oligotróficas de los océanos. Los organismos del fitoplancton en aguas superficiales utilizan el Fe bio-disponible aumentando así la tasa fotosintética. En éste trabajo se investiga la posible fertilización de Fe atmosférico en aguas oligotróficas del Océano Atlántico Norte y del Mar Caribe. Imágenes de satélite (Nivel-3, promedios semanales) de SeaWiFS, MODIS Terra y MODIS Aqua fueron utilizadas para obtener datos de densidad óptica atmosférica (AOT) y concentración de clorofila (Chl_a) desde septiembre 1997 a diciembre 2007. Se presentan resultados para tres áreas del Océano Atlántico Norte y del Mar Caribe, localizadas en 17.5°N, 67.0°W, *Caribbean Time Series Station* (CaTS), 19°N, 57°W, Océano Atlántico Oeste y 20°N, 67°W, Atlántico (Norte de PR). El análisis de serie de tiempo exhibe un patrón estacional con valores máximos de AOT durante el verano. La correlación más fuerte se observó para la estación de Océano Atlántico Oeste con un desfase en tiempo de aproximadamente un mes entre AOT y Chl_a.

La presencia de Fe en muestras de polvo del Sahara fue determinada utilizando técnicas de espectroscopia de reflectancia visible y análisis de elementos traza. El contenido de Fe fue medido en muestras de sedimento de regiones del Norte de África, muestras de polvo colectadas en el mar y muestras de aire filtrado colectadas en PR. El contenido de óxido de Fe mineral se determinó mediante análisis espectral y primera derivada. Todas las muestras presentaron picos distintivos en las primeras derivadas de dos minerales que contienen Fe, hematita y goetita (555-580 para hematita y 435 nm para goetita). Además, la concentración de los elementos traza, Fe y Al, fue medida por la técnica de espectrometría de masas

(*Inductively Coupled Plasma Mass Spectrometry, ICP-MS*). El análisis mostró presencia de Fe en todas las muestras con una mayor concentración en las muestras de tamaños finos (muestras de aire filtradas).

Finalmente, datos de satélite y de campo de AOT y de Chl_a fueron comparados para el Océano Atlántico Norte Tropical durante Marzo 2004 para observar el potencial de las medidas de satélite en estimar propiedades bio-ópticas atmosféricas y oceánicas. Datos de AOT y Chl_a se obtuvieron a bordo del barco NOAA Ronald H. Brown durante la expedición oceanográfica, *Aerosol and Oceanographic Science Expedition* (AEROSE, Febrero 29 - Marzo 26 2004). Estas medidas fueron comparadas con dos productos de Giovanni (*GES DISC Interactive Online Visualization and ANalysis Infrastructure*), AOT (MODIS Aqua 550) y Clorofila Total Asimilada. Los resultados muestran una fuerte relación lineal ($R^2 = 0.86$) entre las medidas de satélite y de campo de AOT. Una fuerte relación ($R^2 = 0.76$) se observó también entre la Chl_a de satélite y de campo, pero el producto de Giovanni subestimó las concentraciones de Chl_a en relación a las medidas en el barco. Además, productos mensuales de Giovanni de AOT y Chl_a se compararon para determinar si se puede establecer una relación entre la entrada de polvo de Sahara y la concentración de Chl_a utilizando datos de Giovanni. Se observó un desfase entre AOT y Chl_a de aproximadamente un mes. Marzo del 2004 coincidió con una de las tormentas de polvo más fuertes para la región. Con el fin de determinar si el evento estaba relacionado a la Oscilación del Atlántico Norte (NAO), se examinaron valores de AOT en relación al índice de NAO de para la estación de Océano Atlántico Oeste (19° N, 57° W). Los resultados mostraron una débil relación lineal entre ambos parámetros.

COPYRIGHT

In presenting this dissertation in partial fulfillment of the requirements for a Doctor of Philosophy degree at the University of Puerto Rico, I agree that the library shall make its copies freely available for inspection. I therefore authorize the Library of the University of Puerto Rico at Mayaguez to copy my dissertation totally or partially. Each copy must include the title page. I further agree that extensive copying of this dissertation is allowable only for scholarly purposes. It is understood, however, that any copying or publication of this dissertation for commercial purposes, or for financial gain, shall not be allowed without my written permission.

A handwritten signature in black ink, appearing to read 'Aurora M. Justiniano Santos', written in a cursive style.

Aurora M. Justiniano Santos
December 27, 2010

Dedication

To my parents, Aurora and Rubén, with all my love and gratitude

To my sisters, Sandra and Jenny, for always holding my hand through difficult times

*To my adorable niece and nephews, Mariela, Rubén, Miguel, Ricardo and Antonio, for
enriching my life with joy, happiness and laughter*

Acknowledgements

I would like to express a sincere gratitude to my advisor, Dr. Roy Armstrong for giving me the opportunity to research under his supervision and for his encouragement and motivation throughout my studies. Special thanks are due to Dr. Yasmín Detrés, who gave me support, guidance, enlightenment and friendship during my years of training. Acknowledgement is also due to Dr. Fernando Gilbes and Dr. José López, for their contribution in the completion of this work. I will like to extend my gratitude to Dr. Vernon Moris from Howard University, Washington DC, for providing useful data and insightful information. Thanks to my Bio-optical Oceanography Laboratory companions and to the administrative staff of the Department of Marine Sciences.

I will also like to acknowledge the Department of General Engineering-Materials Science and Engineering and the Department of Chemistry team, Dr. Perales, Dr. Román, Ms. Diana Sanchez and Mr. Boris Renteria for their contribution in laboratory work and equipment necessary for the fulfillment of this research

Finally, I will like to thank my family, my parents, my sisters, my brothers in law and my loving niece and nephews for their unconditional love and support.

This work was supported by the NOAA Educational Partnership Program with Minority Serving Institutions (EPP/MSI) under cooperative agreements NA17AE1625 and NA17AE1623 (NOAA Center for Atmospheric Sciences).

Table of Content

Abstract.....	ii
Resumen.....	iv
Dedication.....	vii
Acknowledgements.....	viii
List of Tables.....	x
List of Figures.....	xi
Preface.....	1
1. Time series analysis of aerosol optical thickness and chlorophyll concentration in the Tropical North Atlantic Ocean and Caribbean Sea from satellite data.....	4
1.1 Introduction.....	4
1.2 Materials and Methods.....	8
1.3 Results and Discussion.....	16
1.4 Conclusions.....	34
2. Spectral and Trace Element Analysis of African Soils, Saharan Dust Collected at Sea and Filtered Air Samples for Determination of Iron Content in Mineral Dust.....	36
2.1 Introduction.....	36
2.2 Materials and Methods.....	41
2.3 Results and Discussion.....	47
2.4 Conclusions.....	54
3. Satellite and Ground-based Aerosol Optical Thickness and Chlorophyll Concentration in the Tropical North Atlantic Ocean (March, 2004).....	56
3.1 Introduction.....	56
3.2 Materials and Methods.....	60
3.3 Results and Discussion.....	63
3.4 Conclusions.....	73
General Conclusions.....	75
Appendix A: Time Series Plots of Aerosol Optical Thickness and Chlorophyll_a Pigment Concentration for the Three Stations Studied.....	77
Literature Cited.....	80

List of Tables

Table 1.1 Sea-viewing Wide Field-of-view Sensor (SeaWiFS) bands and wavelengths specifications.....	11
Table 1.2 Moderate Resolution Image Spectroradiometer (MODIS) bands specifications...	11
Table 1.3 Analysis of variance for Chl_a measured by MODIS (Aqua and Terra) and SeaWiFS sensors at (a) CaTS, (b) Western Atlantic and (c) Atlantic, North of PR.....	17
Table 1.4 Analysis of variance for AOT measured by MODIS Aqua and Terra) and SeaWiFS sensors at (a) CaTS, (b) Western Atlantic and (c) Atlantic, North of PR.....	18
Table 2.1 Basic statistics: Iron and Aluminum in African soil, Saharan dust collected at sea and filtered air samples.....	53
Table 3.1 Dates and ship position of AOT measurements during AEROSE 2004.....	61
Table 3.2 Dates and ship positions of Chl_a measurements during AEROSE 2004.....	61
Table 3.3 Analysis of variance for ground-based and satellite AOT data.....	65
Table 3.4 Analysis of variance for in-situ and satellite chlorophyll data.....	65

List of Figures

Figure 1 Map showing the areas covered in this study, from North Africa to the Tropical North Atlantic Ocean and the Caribbean Sea.....	3
Figure 1.1 MODIS Aqua Chl_a level 3 weekly-averaged image showing the study site.....	14
Figure 1.2 Chl_a measured by MODIS (Aqua and Terra) and SeaWiFS sensors at (a) CaTS, (b) Western Atlantic and (c) Atlantic, North of PR.....	17
Figure 1.3 AOT measured by MODIS (Aqua and Terra) and SeaWiFS sensors at (a) CaTS, (b) Western Atlantic Ocean and (c) Atlantic, North of PR.....	18
Figure 1.4 Time series plot of AOT measured at CaTS, Western Atlantic Ocean and Atlantic, North of PR (Sept. 1997 – Dec.2007).....	20
Figure 1.5 Time series plots of Chl_a measured at CaTS, Western Atlantic Ocean and Atlantic, North of PR Stations (Sept. 1997 – Dec. 2007).....	20
Figure 1.6 AOT and Chl_a climatology (Sept. 1997 - Dec. 2007) for (a) CaTS, (b) Western Atlantic and (c) Atlantic, North of Puerto Rico.....	21
Figure 1.7 Periodic variations in AOT and Chl_a at (a) CaTS, (b) Western Atlantic and (c) Atlantic, North of Puerto Rico.....	24
Figure 1.8 Time plots of AOT and Chl_a for (a) CaTS, (b) Western Atlantic and (c) Atlantic, North of PR (Sept. 1997- Dec. 2007).....	25
Figure 1.9 Cross-correlation plots for AOT and Chl_a for the (a) CaTS, (b) Western Atlantic and (c) Atlantic, North of PR.....	29
Figure 1.10 AOT (870) and photosynthetically active radiation (PAR) during May-August 2008 at Isla Magueyes field station.....	32
Figure 1.11 Linear fit AOT (870) and PAR during May-August 2008 at Isla Magueyes field station.....	32
Figure 1.12 AOT (870) and UV (305) during May-August 2008 at Isla Magueyes field station.....	33
Figure 1.13 Linear fit AOT (870) and UV (305) during May-August 2008 at Isla Magueyes field station.....	33
Figure 2.1 Soil samples collected from Nigeria, Sudan, Mali and Morocco.....	41

Figure 2.2 Trans-Atlantic Saharan Dust Aerosol and Ocean Science Expedition (AEROSE 2004) cruise tracks.....	41
Figure 2.3 Saharan dust collected at sea during AEROSE 2004.....	41
Figure 2.4 MODIS Terra satellite images (March 2004) showing large Saharan dust storms leaving Africa (a) and moving over the Atlantic Ocean to cover Cape Verde islands (b).....	42
Figure 2.5 Filtered air samples collected at Magueyes Field Station.....	43
Figure 2.6 Thermo Andersen RAAS 2.5-200 air sampler.....	43
Figure 2.7 Iron oxide standard samples: hematite (a) and goethite (b).....	44
Figure 2.8 Percent reflectance spectra (a) and first derivative plots (b) of soil samples collected in North Africa.....	49
Figure 2.9 Percent reflectance spectra (a) and first derivative plots (b) of dust samples collected at sea, during AEROSE 2004.....	49
Figure 2.10 Percent reflectance spectra (a) and first derivative plot (b) for hematite and goethite standards.....	49
Figure 2.11 Percent Fe and Al in soil samples collected from North African.....	52
Figure 2.12 Percent of Fe and Al in Saharan dust samples collected at sea during AEROSE 2004.....	52
Figure 2.13 Percent Fe and Al in filtered air samples collected at Puerto Rico, Magueyes Field Station.....	53
Figure 2.14 Percent Fe in African soil, Saharan dust collected at sea and filtered air samples.....	53
Figure 3.1 MODIS two-day composite true color image showing Saharan dust event leaving North Africa (March 2 -3, 2004).....	59
Figure 3.2 Satellite (Giovanni - MODIS Aqua 550) and ground-based aerosol optical thickness during AEROSE 2004 first leg (a) and second leg (b).....	66
Figure 3.3 Linear relation of daily averaged Giovanni - MODIS Aqua AOT (550) and AEROSE ground-based AOT (870) during March 2004.....	67

Figure 3.4 Giovanni Assimilated Total Chlorophyll (NOBM) and <i>in-situ</i> chlorophyll a concentration (AEROSE 2004).....	68
Figure 3.5 Linear relation of Giovanni Assimilated Total Chlorophyll (NOBM) and <i>in-situ</i> chlorophyll concentration (AEROSE 2004).....	68
Figure 3.6 Time series (Aug. 2002-Dec. 2005) of monthly averaged Giovanni's AOT (550) and Chl_a for the Western Atlantic Ocean.....	69
Figure 3.7 Plot of NAO index and Giovanni's Monthly AOT (550) at Western Atlantic Station for 2004.....	71
Figure 3.8 Plot of the NAO index and Giovanni's Monthly AOT (550) at Western Atlantic Station from 2003 to 2007.....	71
Figure 3.9 Linear relation between the NAO index and Giovanni's monthly AOT (550) data for the Western Atlantic Station (2003 – 2007).....	72
Figure A.1 Time series plot of AOT for CaTS (Sept. 1997 – Dec. 2007).....	75
Figure A.2 Time series plot of Chl_a for CaTS (Sept. 1997 – Dec. 2007).....	75
Figure A.3 Time series plot of AOT for the Western Atlantic Station (Sept. 1997 – Dec. 2007).....	76
Figure A.4 Time series plot of Chl_a for the Western Atlantic Station (Sept. 1997 – Dec. 2007).....	76
Figure A.6 Time series plot of AOT for the North of Puerto Rico Station (Sept. 1997 – Dec. 2007).....	77
Figure A.7 Time series plot of Chl_a for the North of Puerto Rico Station (Sept. 1997 – Dec. 2007).	77

Preface

The high temperatures in the Sahara and Sahel regions of Africa, promotes the heating of surface air resulting in a strong convective activity and the formation of warm dust laden masses of air (Prospero and Carlson, 1972) during the summer time. Strengthening of the easterly winds favor the transport of large quantities of mineral dust toward the Atlantic Ocean and Caribbean Sea in a dry atmospheric air layer called the Saharan Air Layer (SAL). These mineral aerosols travel westwards to the Atlantic and Caribbean region via the Sahara–Sahel Dust Corridor, a zone lying between latitudes 12 °N and 28 °N (Moreno et al., 2006). Mineral aerosols from these desert regions carry nutrients, such as iron (Fe), from continents to the ocean (Claustre et al., 2002). In some parts of the ocean, lack of nutrients and trace metals such as Fe, can be a limiting factor to phytoplankton growth. Mineral aerosols serve as a source of Fe for phytoplankton in surface waters, increasing their rate of primary production (Martin et al., 1994). The importance of the relationship between atmospheric aerosols and oceanic phytoplankton is due to the effect it might have on the carbon cycle. As phytoplankton in surface waters use available Fe, there is an increment in their photosynthetic rate followed by enhanced removal of atmospheric CO₂.

In order to evaluate the relationship between atmospheric aerosols and oceanic primary production it is necessary to carry out large-scale temporal and spatial observations. Satellite-based measurements have been proven to be an excellent tool to study large-scale atmospheric aerosols and chlorophyll concentrations. Dust clouds can be tracked from their source to thousands of km away using satellite observations, improving the knowledge of the distribution of aerosols in the atmosphere (Myhre et al., 2005). Likewise, ocean color measured from space provides global information on bio-optical properties and subsurface

oceanographic parameters such as chlorophyll concentration (Darecki and Stramski, 2004). However, to accurately study atmospheric dust distribution and their impacts on the environment, it is necessary to integrate continuous satellite observations with ground-based instruments and field experiments (Kaufman et al., 2002).

This study is intended to investigate the possible Fe fertilization of surface waters of the Tropical North Atlantic Ocean and Caribbean Sea by mineral dust from the Saharan and Sahel regions using satellite data. Based on this main objective, the dissertation has been divided into three chapters, each prepared following the guidelines commonly used in scientific publications. Chapter one examines the relationship between the aerosol dust plume traveling from Africa toward the Tropical North Atlantic Ocean and an increase in phytoplankton's biomass using satellite based measurements. The second chapter estimates Fe element content in desert dust particles, from their source region in North Africa, through their atmospheric transport through the North Atlantic Ocean and as they reach remote areas from their origin. Finally a third chapter evaluates the potential of satellite measurements in describing both, atmospheric and oceanographic processes and complements satellite data with ground-based observations. The study was carried out at selected areas of the Tropical North Atlantic Ocean and Caribbean Sea, which are subjected to strong seasonal inputs from Saharan mineral aerosols (Figure 1). The region is of particular interest since it is classified as oligotrophic and as having low dissolved Fe concentrations.

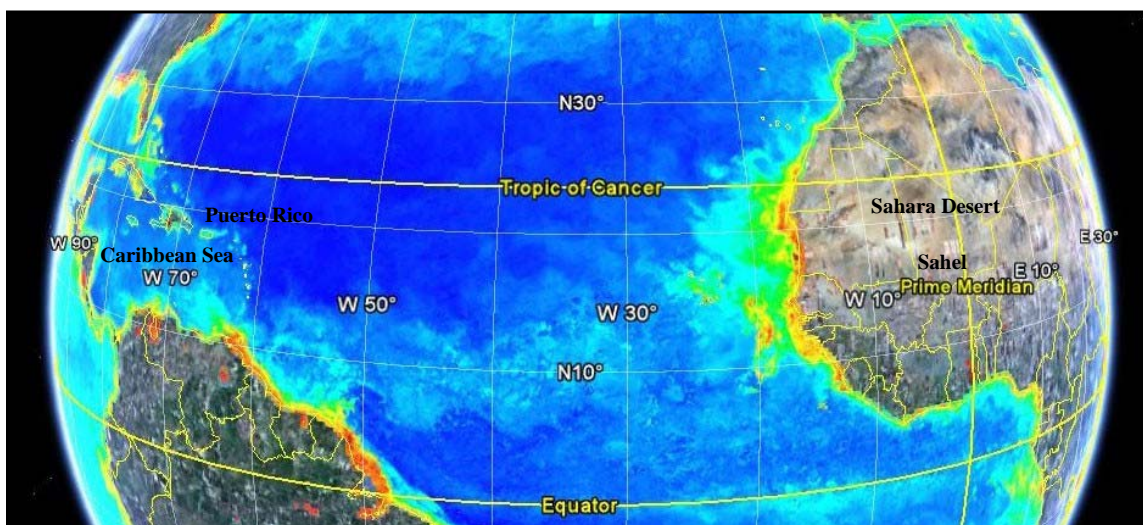


Figure 1 Map showing the areas covered in this study, from North Africa to the Tropical North Atlantic Ocean and the Caribbean Sea (Google Earth Image).

1. Time series analysis of aerosol optical thickness and chlorophyll concentration in the Tropical North Atlantic Ocean and Caribbean Sea from satellite data

1.1 Introduction

The atmosphere is an important pathway for the transport and dispersion of nutrients, minerals, microorganisms and trace metals from continents to the oceans. Atmospheric dust particles originating in the arid and semi arid regions of the world are known to be principal sources of mineral dust. Particles traveling from the Sahara desert to oligotrophic regions of the ocean provide an important supply of nutrients such as iron for oceanic phytoplankton, affecting the biogeochemistry of the area (Prospero et al., 1981; Claustre et al., 2002). According to the *Iron Hypothesis* formulated by Martin (1994) the availability of iron in the ocean has an effect on the primary production of a given region. Many studies have also demonstrated the importance of trace elements in regulating phytoplankton growth and limiting oceanic primary production (Martin et al., 1991; Lenes et al., 2001; Kustka et al., 2002; Bonnet and Guieu, 2004; Jickells et al., 2005; Moore et al., 2006). There is an increasing interest in the interaction between iron input and phytoplankton ecosystem dynamics due to the effect it might have on climate change. Iron is an important micronutrient and deposition of iron from mineral aerosols can impact the carbon cycle (Mahowald et al., 2005). As phytoplanktonic organisms in the ocean's surface use iron from aerosol particles their rate of photosynthesis and primary production may increase, resulting on enhanced removal of carbon dioxide from the atmosphere.

Observations of African dust concentration, transport, and deposition have been carried out using satellite data since the 1970s. Values of 240 ± 80 Tg of dust particles have been

reported to be transported annually from Africa toward the ocean, from which 140 ± 40 Tg are deposited in the North Atlantic Ocean and approximately 50 Tg reach the Caribbean Sea (Kaufman et al., 2005). The frequency and magnitude of dust input is influenced by season, source area, climate, human land disturbance, local and regional scale weather and global atmospheric circulation (Bonnet et al., 2005). In many regions of the world's oceans, climatic fluctuations in atmospheric dust deposition impact the marine carbon cycle. High dust deposition mitigates iron limitation increasing nitrogen fixation, primary production and oceanic CO₂ uptake from the atmosphere (Moore et al., 2006). In the Tropical North Atlantic Ocean primary production in surface waters is limited by lack of bio-available nitrogen, which is co-limited by insufficient iron concentrations (Mills et al., 2004). Even though there is considerable amount of molecular nitrogen (N₂), it cannot be used directly by photosynthetic organisms, which require nitrogen in the form of nitrate (NO₃⁻) or ammonium (NH₄⁺). Nitrogen fixation by diazotrophic organisms provides a source of usable nitrogen for photosynthesis. In the Tropical North Atlantic Ocean, the diazotrophic cyanobacterium *Trichodesmium spp.* is one of the principal components of the phytoplankton and N₂ fixation by this organism is a major resource of new nitrogen in the region (Capone et al., 2005). Measurements of abundance and numerous observations indicate that *Trichodesmium spp.* is the most important primary producer in the Tropical North Atlantic Ocean (Carpenter and Romand, 1991). Studies of N₂ fixation in surface waters of the North Atlantic Ocean have shown that both *Trichodesmium* abundance and N₂ fixation rates correlated positively with dissolved Fe, supporting the idea that Fe influences N₂ fixation (Moore et al., 2009). An increase in primary productivity due to N₂ fixation by these organisms increases oceanic

sequestration of carbon and may have a significant effect on global climate (Kustka et al., 2002).

However, even though atmospheric iron input increases the concentration of iron in seawater, the ocean's biogeochemistry is affected by soluble Fe and not by dust flux to the ocean. Soluble bio-available Fe in marine water, which is defined as the portion of Fe present in the form of ferrous ion (Fe^{2+}), tends to be in low concentrations. Most of the iron that reaches the ocean from external sources is in the form of ferric ion (Fe^{3+}) and must be reduced to Fe^{2+} . This transformation is carried out mainly by photo-reduction and depends on the time the dust particles spend in contact with the atmosphere and in the surface waters. Experiments describing the dissolution processes of iron in seawater exhibit an increase in the dissolved iron concentration after 7 days of adding dust particles (Bonnet and Guieu, 2004). Other studies show that the dissolved flux represents 4-17% of the total atmospheric flux of iron (Guieu et al., 2002). Iron's solubility in seawater is affected by other factors such as suspended particle concentration and aerosol source. Also, it has been observed that Fe is highly insoluble under oxidizing conditions and under conditions of pH higher than 4 (Jickells et al., 2005). Changes in aerosol pH caused by wetting and drying cycles associated with repeated passage of aerosol particles through clouds has been observed to enhance Fe solubility (Baker et al., 2006).

In order to determine the effects of iron input in the biogeochemistry of the ocean it is necessary to evaluate long-term records of atmospheric aerosols and chlorophyll pigment concentrations (Chl_a). Satellite-based measurements provide the only source of data for large-scale regional and global observations. At the end of 1999, the launch of the first Moderate Resolution Imaging Spectroradiometer (MODIS) instrument made possible

quantitative and systematic measurements of dust transport for the Atlantic Ocean (Kaufman et al., 2005). Dust clouds are observable from satellites and can be tracked from their source to thousands of kilometers away as they cross the oceans. Comparisons between aerosol and Chl_a concentrations using satellite data have presented periods of elevated aerosol signals followed by increase in phytoplankton biomass, suggesting a connection between aerosol load and phytoplankton growth (Stegmann, 2000).

Aerosol concentration can be obtained by the satellite-mapped product, aerosol optical thickness (AOT), which quantifies atmospheric suspended particles and the degree to which they prevent the transmission of light. Likewise, ocean color is a unique property that can be measured from space and provides global information on subsurface oceanographic parameters (Darecki and Stramski, 2004). Since Chl_a absorbs more blue and red light than green, the spectrum of backscatter sunlight from the oceans shifts from deep blue to green as the concentration of phytoplankton increases (O'Reilly et al., 1998). Therefore Chl_a concentration, which alters the color of the ocean, can also be determined from satellite data.

This work aims to investigate the possible iron fertilization of oligotrophic Tropical North Atlantic and Caribbean waters using satellite data from SeaWiFS (Sea-viewing Wide Field-of-view Sensor) and MODIS (on board of Terra and Aqua satellite). Level 3 weekly averaged images from September 1997 through December 2007 were used to evaluate long-term records of AOT and Chl_a for three areas in the North Atlantic Ocean and the Caribbean Sea. The study area is subjected to strong seasonal inputs from Saharan mineral aerosols. This region is of particular interest since it is classified as oligotrophic and as having very low dissolved Fe concentrations. Changes in Fe flux to the Tropical North

Atlantic Ocean and Caribbean Sea may play a role in climate change, influencing primary production and therefore the carbon cycle.

1.2 Materials and Methods

Study Site

The Tropical North Atlantic Ocean and the Caribbean Sea have been traditionally classified as oligotrophic low productive systems. The presence of a permanent thermocline inhibits mixing between superficial, low nutrient waters with deeper waters rich in nutrient concentrations. However, studies have revealed that the region undergoes pronounced seasonal variation in phytoplankton population density (González et al., 2000). Observations and field studies have proven that this region is affected by external and seasonal events that alter the amount of nutrients present in the region. For example, the Caribbean is a semi-enclosed tropical sea influenced by an annual discharge of the Amazon and Orinoco Rivers (Müller-Karger et al., 1989). Satellite images from SeaWiFS have shown the intrusion of waters from the Orinoco River during fall and from the Amazon River during spring–summer into the eastern Caribbean Sea (Gilbes and Armstrong, 2004). The area is also affected during winter–spring by a strong coastal upwelling in Venezuela produced by the trade winds, supplying large concentrations of nutrients to surface waters. Studies have shown high pigment concentrations during the months of January through May, along the continental margin, where upwelling occurs (Müller-Karger et al., 1989).

During summer the Tropical North Atlantic Ocean and the Caribbean Sea may also be affected by the passing of hurricanes, which develop off the west coast of Africa. The turbulent events associated with the strong cyclonic surface winds of hurricanes are known to provoke mixing of waters, transporting subsurface waters with increased nutrient

concentrations to the surface. In coastal areas, hurricanes also have an effect on increasing precipitation and runoff, which in turn increases the nutrients. For example, increased concentrations of Chl_a around Puerto Rico following Hurricane Georges was observed from SeaWiFS images as a result of high river discharge of nutrient rich waters (Gilbes et al., 2001). Finally, mineral dust transported through the atmosphere supplies an important amount of nutrients to the open ocean (Prospero et al., 2002). It has been observed that atmospheric transport from continents is probably the dominant source of nutrient Fe in the photic zone (Duce and Tindale, 1991). Particles moving toward the North Atlantic Ocean and Caribbean Sea from the Saharan desert are, therefore, an important source of fertilization for this region. Saharan dust is transported along different paths, from which the westward flow over the North Atlantic Ocean is the most voluminous one (Goudie and Middleton, 2001). The areas selected for this study are of particular interest since they are subjected to the strong seasonal input from Saharan mineral aerosols.

Instrument Description – Satellite Sensors

The Sea-viewing Wide Field-of-view Sensor (SeaWiFS) was launched on the OrbView-2 spacecraft in August 1997 with the purpose of providing quantitative data on global ocean bio-optical properties. SeaWiFS measures atmospheric radiance in eight narrow spectral bands (Table 1.1). The bands span from the visible to the near infra-red parts of the spectrum centered on 412, 443, 490, 510, 555, 670, 765 and 865 nm, with a spectral resolution of 20 nm for wavelengths smaller than 700 nm and 40 nm for wavelengths larger than 700 nm (Lavendera et al., 2005).

The Moderate Resolution Imaging Spectroradiometer (MODIS) onboard the NASA Terra and Aqua satellites is a multipurpose instrument designed for the global remote sensing of

land, ocean and atmosphere (Gao et al., 2007). MODIS was developed in part to study the importance of global observations in marine ecosystem research. It was designed to serve the scientific community with respect to ocean color and to obtain consistent observations useful for understanding the role of the ocean in the earth system and in the global carbon cycle (Esaías et al., 1998). The instrument allows monitoring of large-scale spatial and temporal analysis, with a 2330 km viewing swath width that provides almost complete global coverage in one day. It acquires data in 36 high spectral resolution bands (Table 1.2) between 0.415 and 14.235 μm with spatial resolutions of 250 m, 500 m and 1000 m (Savtchenko et al., 2004).

NASA's Earth Observing System (EOS) launched Terra on December 18, 1999. It orbits around the Earth from north to south crossing the equator in the morning. Aqua, formerly named EOS PM, was launched on May 4, 2002 and orbits south - north across the equator in the afternoon.

Table 1.1 SeaWiFS instrument bands and wavelengths.

Band	Wavelength (nm)	Band	Wavelength (nm)
1	402-422	5	545-565
2	433-453	6	660-680
3	480-500	7	745-785
4	500-520	8	845-885

(<http://oceancolor.gsfc.nasa.gov/SeaWiFS/SEASTAR/SPACECRAFT.html>)

Table 1.2 MODIS Bands Specifications:

Primary Use	Band	Bandwidth (nm)	Primary Use	Band	Bandwidth (µm)
Land/Cloud Aerosols Boundaries	1	620 - 670	Surface/Cloud Temperature	20	3.660 - 3.840
	2	841 - 876		21	3.929 - 3.989
Land/Cloud/Aerosols Properties	3	459 - 479		22	3.929 - 3.989
	4	545 - 565		23	4.020 - 4.080
	5	1230 - 1250	Atmospheric Temperature	24	4.433 - 4.498
	6	1628 - 1652		25	4.482 - 4.549
	7	2105 - 2155	Cirrus Clouds Water Vapor	26	1.360 - 1.390
	8	405 - 420		27	6.535 - 6.895
Ocean Color/ Phytoplankton/ Biogeochemistry	9	438 - 448		28	7.175 - 7.475
	10	483 - 493	Cloud Properties	29	8.400 - 8.700
	11	526 - 536	Ozone	30	9.580 - 9.880
	12	546 - 556	Surface/Cloud Temperature	31	10.780 - 11.280
	13	662 - 672		32	11.770 - 12.270
	14	673 - 683	Cloud Top Altitude	33	13.185 - 13.485
	15	743 - 753		34	13.485 - 13.785
	16	862 - 877		35	13.785 - 14.085
				36	14.085 - 14.385
Atmospheric Water Vapor	17	890 - 920			
	18	931 - 941			
	19	915 - 965			

(<http://modis.gsfc.nasa.gov/about/specifications.php>)

Since the 1970s, a variety of bio-optical algorithms have been developed to estimate chlorophyll concentration using ocean radiance data (O'Reilly et al., 1998). The algorithm used to estimate Chl_a from SeaWiFS data relates band ratios to chlorophyll with a single polynomial function. It uses the maximum band ratio (MBR) determined as the greater of the R_{rs} 443/555, 490/555 or 510/555 values (O'Reilly, 2000). The fourth order polynomial algorithm, known as OC4, is given by the following equation:

$$\text{Chl}_a = 10^{(0.366 - 3.067R_S + 1.930R_S^2 + 0.649R_S^3 - 1.532R_S^4)} \quad (\text{a})$$

$$\text{Where } R_S = \log_{10} [\max R_{rs} 443, 490, 510 / R_{rs} 555]$$

Likewise, MODIS Chl_a algorithm, OC3M, makes use of a MBR but only incorporates 443 and 490. MODIS is currently producing SeaWiFS analog chlorophyll product that employs the algorithm parameterized with the same data set used for the SeaWiFS OC4 algorithm (Campbell, 2005).

$$\text{Chl} = 10^{(0.2830 - 2.573 R_{3M} + 1.457R_{3M}^2 + 0.659R_{3M}^3 - 1.403 R_{3M}^4)} \quad (\text{b})$$

$$\text{Where } R_{3M} = \log_{10} [\max 443/550 > 490/550]$$

Differences in the Chl_a retrievals between these two algorithms can approach 25% in turbid water (O'Reilly, 2000). As turbidity increases, the selected maximum-band migrates from shorter (blue) to longer (green) wavelengths. In the most turbid water, OC4 selects 510, while OC3 remains at 490. This generates differences in the functional form of each algorithm, which leads to differing estimated Chl_a in turbid water.

For aerosol concentration remote sensors provide the satellite-mapped product called aerosol optical thickness (AOT), which quantifies atmospheric suspended particles and the degree to which they prevent the transmission of light. The parameter is a by-product resulting from atmospheric correction measurements, which are essential to model and

remove atmospheric and oceanic scattering effects from the total radiance measurements (Gordon and Wang, 1994).

The atmospheric correction algorithm developed by Gordon and Wang (1994) defines total reflectance ($\rho_t(\lambda)$) as the sum of the contributions supplied by water ($\rho_w(\lambda)$), Rayleigh reflectance due to backscattering by atmospheric molecules ($\rho_r(\lambda)$), reflectance from backscatter by atmospheric aerosols ($\rho_a(\lambda)$), reflectance from a combination of molecular and aerosol scattering ($\rho_{ra}(\lambda)$), reflectance by white-capping ($\rho_{wc}(\lambda)$) and sunglint ($\rho_g(\lambda)$):

$$\rho_t(\lambda) = \rho_r(\lambda) + [\rho_a(\lambda) + \rho_{ra}(\lambda)] + t(\lambda) \rho_{wc}(\lambda) + t(\lambda) \rho_g(\lambda) + t(\lambda) \rho_w(\lambda) \quad (c)$$

The concentration of the aerosols and their optical properties need to be determined in order to solve the $[\rho_a(\lambda) + \rho_{ra}(\lambda)]$ term. This aerosol information is derived by extrapolation from the near infrared (IR) to the visible part of the spectrum (Gao et al., 2007). Aerosol radiance contribution is then known and can be removed. In order to characterize aerosol optical properties, SeaWiFS uses two near infrared bands centered at 765 and 865 nm which are then extrapolated to different parts of the spectrum (Wang, 2000). MODIS, with much more spectral diversity, has the ability to retrieve aerosol optical thickness with greater accuracy (Remer et al., 2005). For AOT characterization it uses bands 15 and 16 with bandwidths ranging from 743 to 753 and 862 to 877 nm, respectively.

Methodology

Remote sensed image data were used to analyze values of AOT and Chl_a from September 1997 through December 2007. SeaWiFS (1997-1999), MODIS Terra (2000-2003) and MODIS Aqua (2004-2007) level 3 weekly averaged images were obtained from NASA-Goddard Space Flight Center, ocean color web (<http://oceancolor.gsfc.nasa.gov>). An analysis of variance (AOV) was performed to evaluate if any variability existed between the data acquired from the three sensors using images of Chl_a from 2007 and of AOT from 2003.

A time series analysis was carried out for three areas in the Tropical North Atlantic Ocean and Caribbean Sea. Station 1 was set at the Caribbean Time Series Station (CaTS) located approximately 26 nautical miles off the southwestern coast of Puerto Rico (17°N , 67°W) in the Caribbean Sea. Station 2 was situated in the Western Atlantic Ocean (19°N , 57°W) and Station 3 was located in the Atlantic Ocean North of P.R at 20°N , 67°W (Figure 1.1).

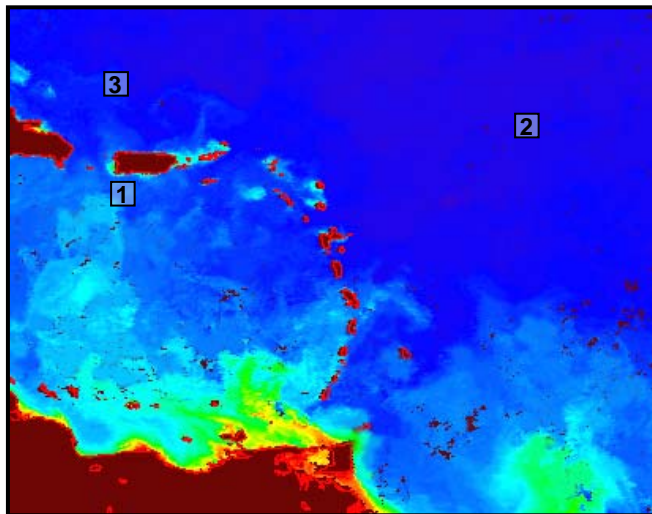


Figure 1.1 MODIS Aqua Chl_a level 3 weekly-averaged image showing the study sites. Station 1 was located at 17.5°N , 67°W (CaTS), Station 2 at 19°N , 57°W (Western Atlantic) and Station 3 at 20°N , 67°W (Atlantic, North of PR).

The images were processed in LINUX platform using the image analysis package *SeaWiFS Data Analysis System* (SeaDAS), design for processing, display, analysis, and quality control of ocean color data. A subset of the image containing the three boxes was used to facilitate the processing (latitude range: 25°N, 5°S, long. range: -70°W, -50°E). For each site, boxes of 15 x 15 pixels were selected for the analysis. The valid range of values used were 0.01- 25 (mg m^{-3}) for chlorophyll pigment concentration and 0.001 to 0.5 for aerosol optical thickness. Mean values of each 15 x 15 pixels data set for Chl_a and AOT were retrieved for further analysis.

A time series analysis was carried out by means of the Math Works, matrix laboratory software (MATLAB) to understand the underlying context of the data and to make predictions of future events. The analysis was executed for AOT and Chl_a to examine and compare variations of both parameters with respect to each other and with respect to time. The data was plotted as a function of time to see important features such as periodicities, seasonality and to observe how the signals changed over the studied period. A spectral analysis or periodogram was used to determine the frequencies of the periodic variation in the data and to examine at which frequencies these variations were strong or weak.

Finally, a cross-correlation analysis was carried out to measure the degree of the linear relationship between the two variables; to determine if an increase in AOT results in an increase in Chl_a. Also, it provided information on the relative time lag between both signals and if there was a time delay in the system.

1.3 Results and Discussion

MODIS and SeaWiFS comparison:

Chl_a measured by MODIS (Terra and Aqua) and SeaWiFS were compared at selected stations (Figures 1.2). Close similarity is observed between the values obtained by the three sensors for the studied area. An analysis of variance for Chl_a measured by the three sensors at each station presented no significant differences between sensors for both CaTS and Western Atlantic Ocean (Table 1.3). This was not the case for the North Atlantic Station, where significant differences were noted.

The same analysis was carried out for values of AOT (Figure 1.3). The analyses of variance for AOT measured at the studied stations are shown in Table 1.4. In this case, all three stations present no significant difference between values measured by the three sensors.

These results suggest that even though there are some variations in the algorithms used by each sensor to calculate Chl_a and AOT, there is no significant difference in the values obtained for AOT at our three stations and between the values of Chl_a at two of our three stations. Therefore, the 11 years time series analysis was performed using data from MODIS Aqua, Terra and SeaWiFS sensors.

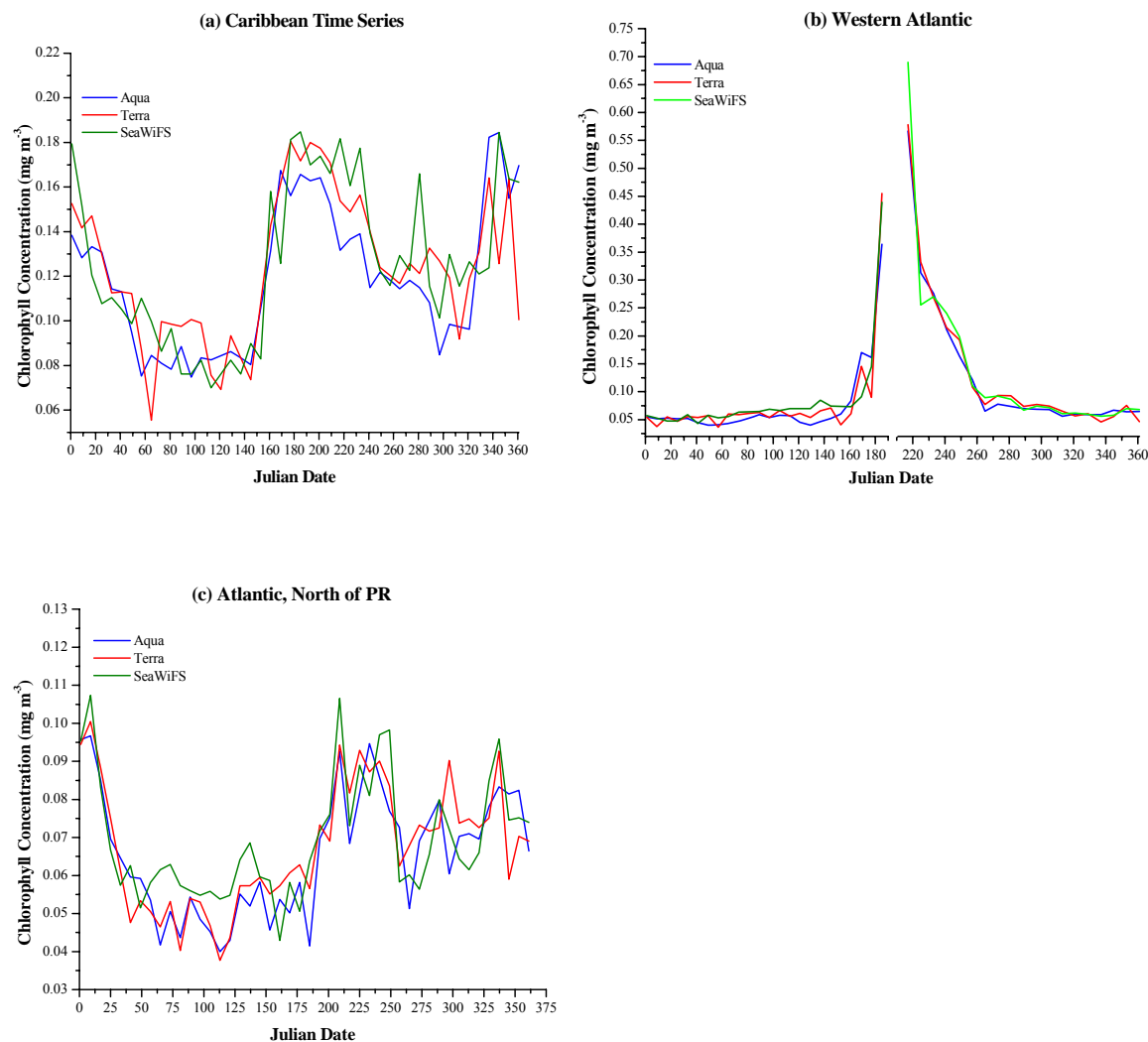


Figure 1.2 Chlorophyll_a pigment concentration measured by MODIS Aqua, Terra and SeaWiFS sensors at (a) CaTS, (b) Western Atlantic and (c) Atlantic, North of PR.

Table 1.3 Analysis of variance: Chlorophyll Concentration

a. CaTS					b. Western Atlantic				
Source	SS	df	MS	F	Source	SS	df	MS	F
Treatment	0.00126	2	0.000628564	2.68	Treatment	0.00196	2	0.000982	2.92
Block	0.12640	45	0.002808833		Block	1.53230	42	0.036483	
Error	0.02109	90	0.000234369		Error	0.02822	84	0.000336	
Total	0.14875	137			Total	1.56249	128		

c. Atlantic, North of PR				
Source	SS	df	MS	F
Treatment	0.00030	2	0.000151444	3.50 *
Block	0.03051	45	0.000677916	
Error	0.00389	90	0.000043	
Total	0.03470	137		

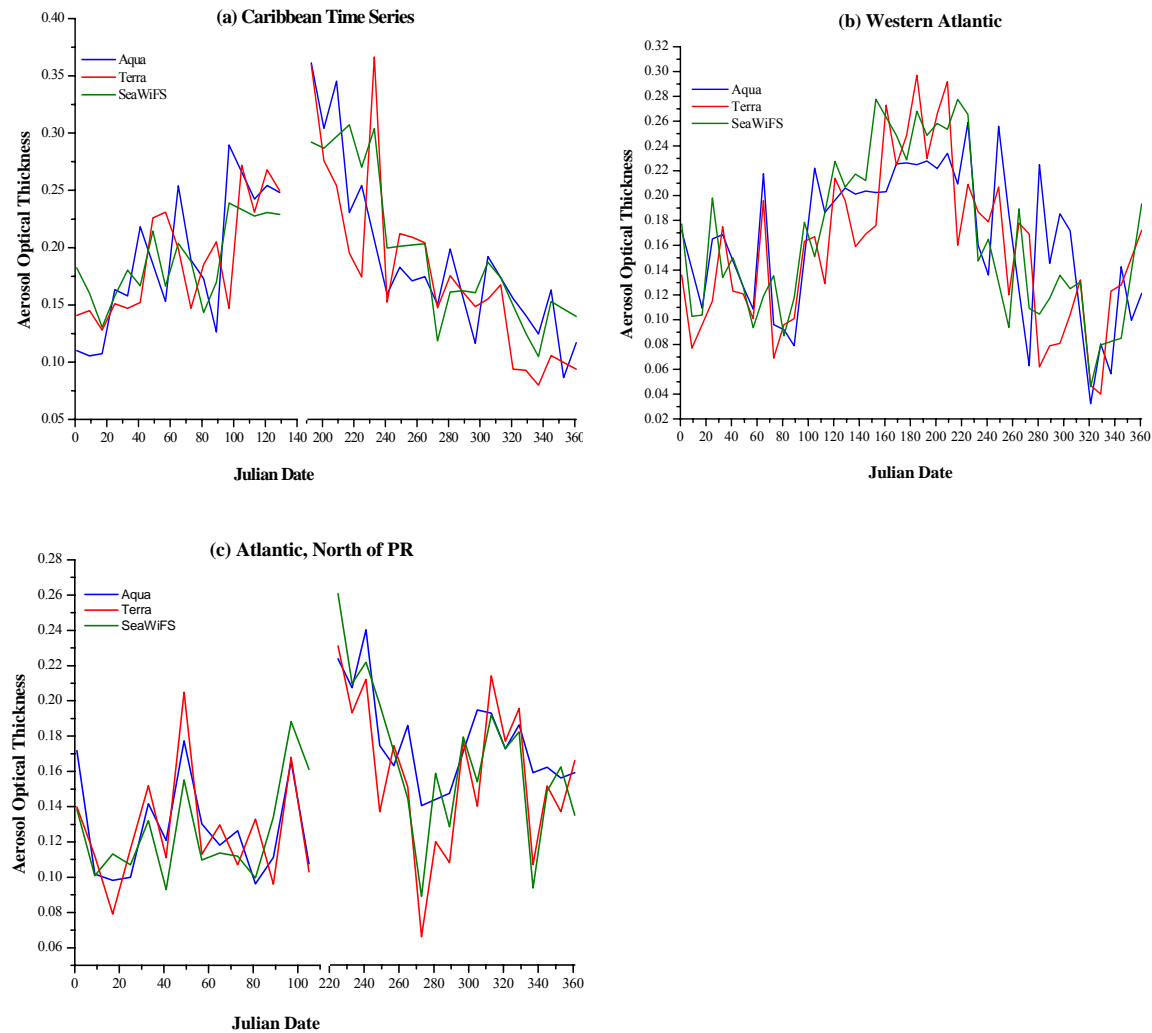


Figure 1.3 Aerosol optical thickness (AOT) measured by MODIS Aqua, MODIS Terra and SeaWiFS sensors at (a) CaTS, (b) Western Atlantic Ocean and (c) Atlantic, North of PR.

Table 1.4 Analysis of variance: Aerosol Optical Thickness

a. CaTS

Source	SS	df	MS	F
Treatment	0.002333	2	0.001167	1.14
Block	0.373105	38	0.009819	
Error	0.077842	76	0.001024	
Total	0.45328	116		

b. Western Atlantic

Source	SS	df	MS	F
Treatment	0.002521	2	0.00126	1.10
Block	0.413469	45	0.009188	
Error	0.10339	90	0.001149	
Total	0.51938	137		

c. Atlantic, North of PR

Source	SS	df	MS	F
Treatment	0.001664	2	0.000832	2.53
Block	0.129649	31	0.004182	
Error	0.02040	62	0.000329	
Total	0.15171	95		

α 0.05

Time Series Analysis

Time series plots of AOT and Chl_a for the three selected stations are displayed in Figures 1.4 and 1.5 respectively (for individual plots of AOT and Chl_a at each station refer to Appendix A). The data, covering the studied period from September 1997 through December 2007, show important features such as periodicity and seasonality. Both parameters repeated themselves in systematic intervals over time, revealing a marked seasonal component. Maximum values for AOT and Chl_a pigment concentration occurred during the summer months (July-August) while minimum values were observed during the winter (December-February).

The pattern encountered for both parameters corresponds to the strong seasonal variation in the occurrence of African dust storms which take place primarily from late spring through early fall. Transport of Saharan dust particles is active all year but reaches its peak during the summer time over the North Atlantic Ocean between the desert, the Caribbean, and the United States. High summer temperatures promote the formation of dust storms and strengthening of the easterly winds, which drives the transportation of large quantities of mineral aerosols. Also, there is a latitudinal variation in the transport of Saharan dust particles across the North Atlantic Ocean, which responds to seasonal differences in the direction of the easterly winds. During the summer the Trade winds move toward the north (latitudes of approximately 20°N), while during the winter it tends toward lower latitudes (5°N). Climatology graphs for the three stations show evidence of a seasonal variability in AOT that responds to a maximum in summer dust input (Figures 1.6). The same was observed for Chl_a values at CaTS and Western Atlantic Ocean. In the case of the Atlantic, North of PR, Chl_a values presented little seasonality and relatively lower values.

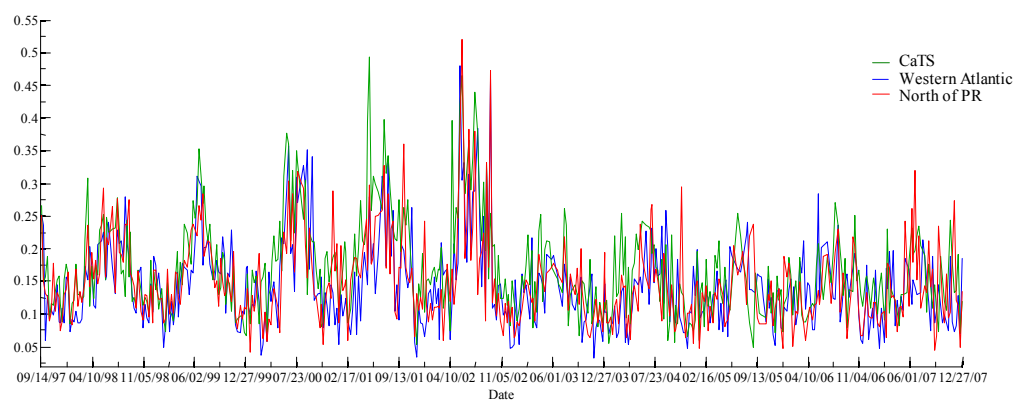


Figure 1.4 Time Series plot of AOT for CaTS, Western Atlantic Ocean and Atlantic, North of PR Stations (Sept. 1997 – Dec. 2007).

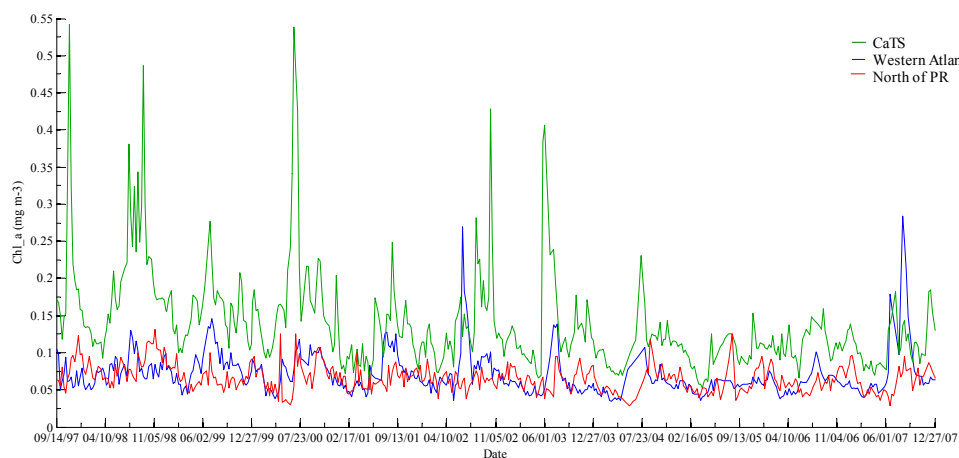


Figure 1.5 Time series plots of Chl_a for CaTS, Western Atlantic Ocean and Atlantic, North of PR Stations (Sept. 1997 – Dec. 2007).

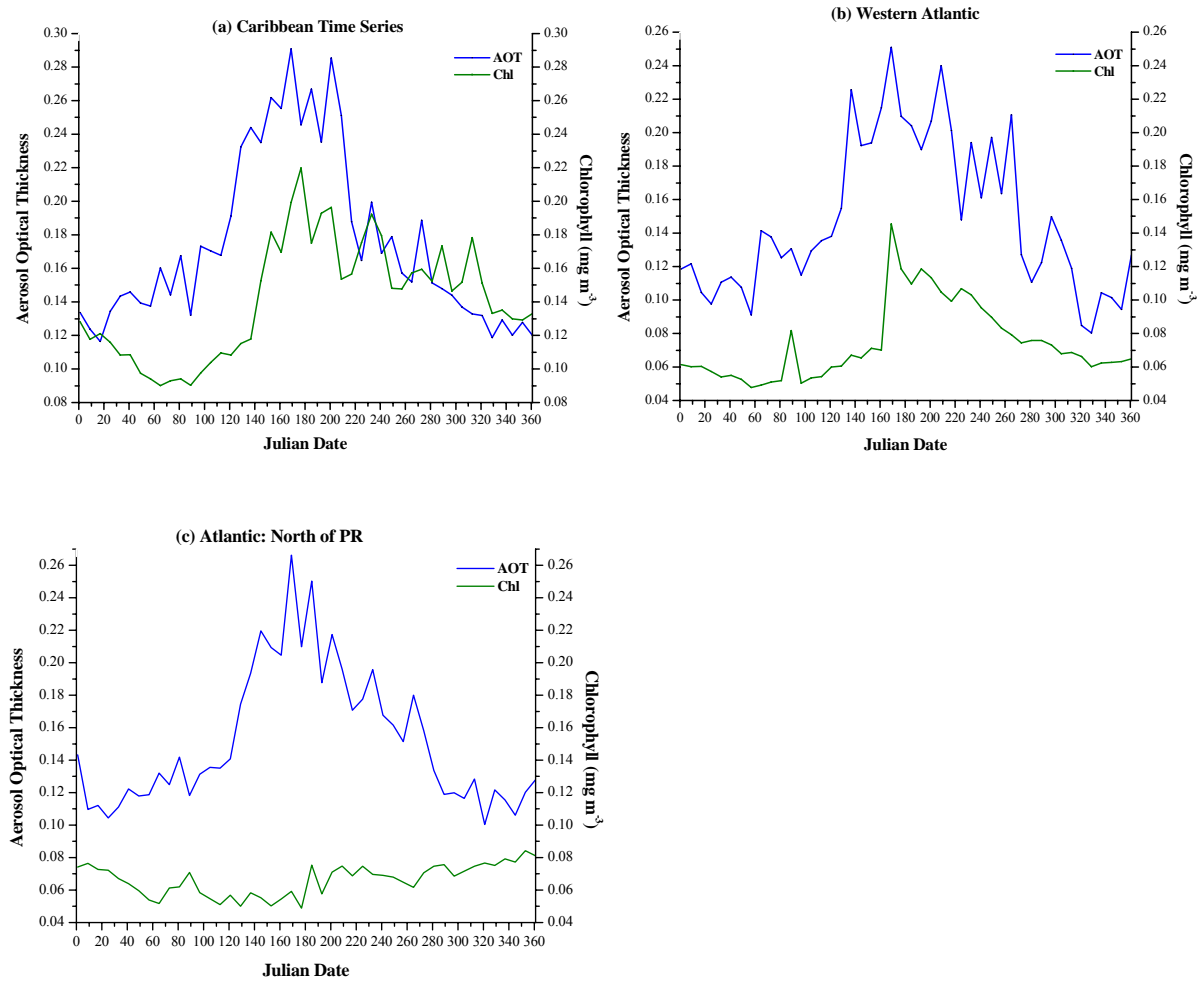


Figure 1.6 AOT and Chl_a climatology from September 1997 through December 2007 for (a) CaTS, (b) Western Atlantic & (c) Atlantic, North of Puerto Rico Stations

The Western Atlantic site, located far from coastal influences and situated directly in the path of the African dust storms, shows a more defined seasonal pattern for both parameters (Figures A.3 and A.4, Appendix A). The lowest values for Chl_a concentration were observed at the Atlantic, North of Puerto Rico Station, situated at a northwestern location and connected to southern waters of the Sargasso Sea. On the other hand, from Figure 1.5 it is evident that the values of Chl_a encountered at CaTS were much higher than those found at the other two stations. Higher values at CaTS might be the consequence of external factors due to inputs from riverine nutrient sources. Of special interest is the effect of the Amazon

and the Orinoco rivers on the adjacent ocean. Observations have shown regular seasonal changes in the patterns of dispersal of water from these rivers toward the western tropical Atlantic (Chuanmin et al., 2004). Studies using NASA's Coastal Zone Color Scanner (CZCS) revealed that the Amazon River discharge is carried northwestward towards the Caribbean Sea from February to May (Muller-Karger et al., 1998). Other studies using absorption and fluorescence spectroscopy emphasize the significant effect of the Orinoco River discharge on the optical properties the Caribbean Sea (Del Castillo et al., 1999). Also, investigations conducted at CaTS show the seasonal effects of river discharge incoming from the Orinoco and Amazon Rivers on Chl_a concentrations (Gilbes and Armstrong, 2004). During the fall season, an increase in the Orinoco River discharge produces an intrusion of its waters toward the Caribbean Sea and during the spring-summer a similar effect is observed with waters from the Amazon River. Also, during winter-spring the eastern Caribbean is influenced by a strong coastal upwelling in Venezuela that supplies large concentrations of nutrients to surface waters. The optical complexity arising from riverine inputs may also contribute to the Chl_a variability observed using satellite data at CaTS.

The frequencies of the periodic variations in the data for both parameters were further evaluated at each site. Periodograms for AOT and Chl_a showed a maximum energy peak at a frequency of approximately 0.3×10^{-7} (cycles/second), which is equivalent to a period of nearly one year. The same peak was observed for both parameters at CaTS (Figure 1.7.a) and the Western Atlantic Station (Figure 1.7.b). The Atlantic, North of PR station showed the same frequency for AOT but presented almost no signal for Chl_a. Even with high variation in AOT values, Chl_a concentration at this station remained constant over the studied period (Figure 1.7.c).

For the other two stations, the periodic component in the data resulted in an annual variation for both parameters. There is high variability in AOT and Chl_a concentration, which is associated to fluctuations that occur in a period of one year, observed for the three stations. The Tropical North Atlantic Ocean is therefore exposed to cyclic annual dust events, with maximum mineral dust transport occurring each summer and minimal dust concentration present during the winter. The same annual fluctuations were observed for Chl_a pigment concentration, suggesting a relationship between both parameters. This relationship can be observed through time plots, comparing both parameters throughout the studied period (Figures 1.8). Episodes of elevated aerosol dust loading were followed by an increase in Chl_a suggesting a link between mineral dust particles and chlorophyll pigment concentration.

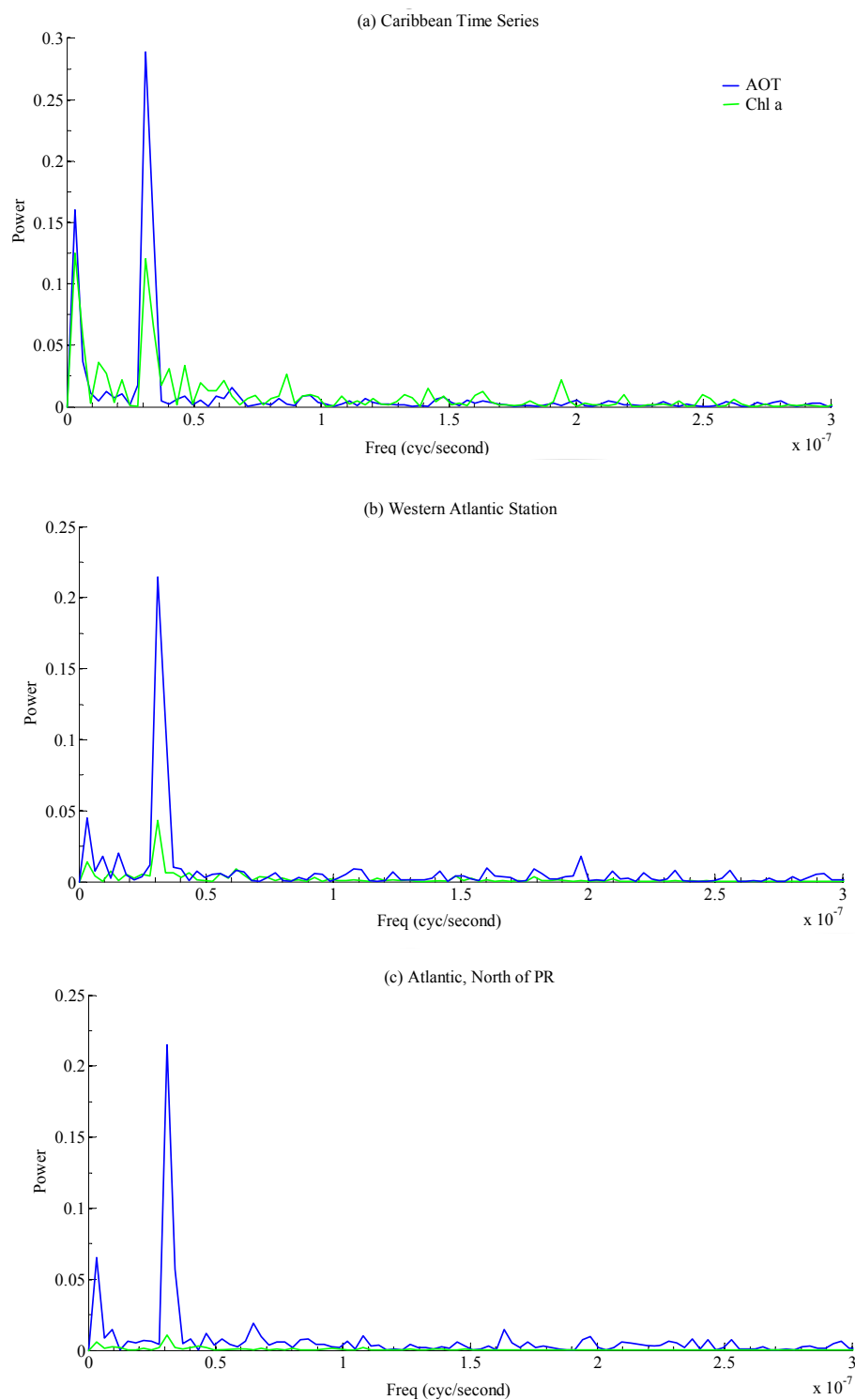


Figure 1.7 Periodic variations in aerosol optical thickness and chlorophyll concentration at (a) CaTS, (b) Western Atlantic and (c) Atlantic, North of Puerto Rico.

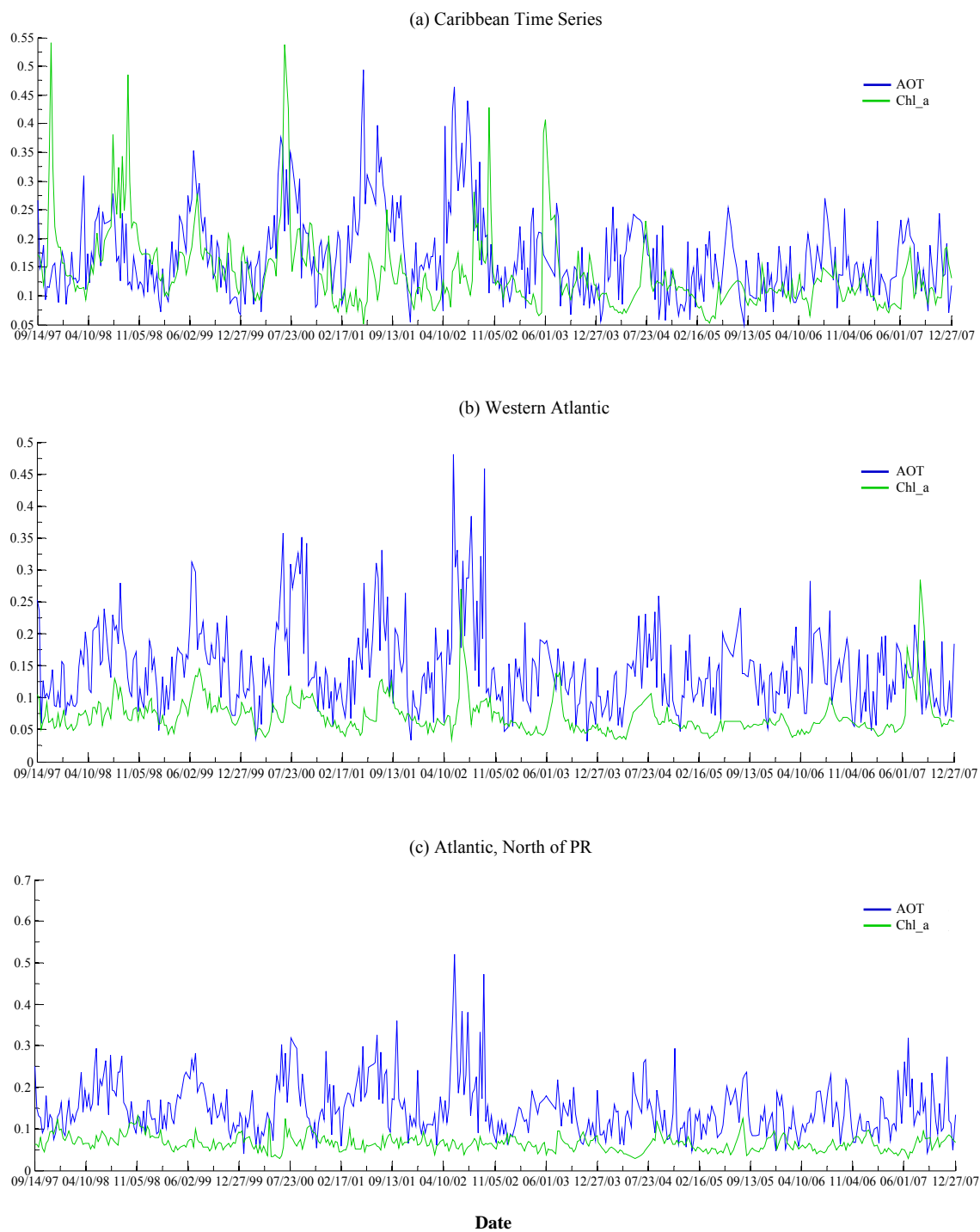


Figure 1.8 Time plots of AOT and Chl_a (mg/m^3) for (a) CaTS, (b) Western Atlantic and (c) Atlantic, North of PR (September 1997 through December 2007).

The relationship between AOT and Chl_a was further examined by cross correlation analysis, which measured how much the two variables changed together and provides the time lag between both signals. The correlation analysis for CaTS is presented in Figure 1.9.a. The correlation coefficients for this station were statistically less significant than for the Western Atlantic Station, with two time lags observed (2 weeks: $r = 0.32$ and 4 weeks: $r = 0.33$). The variability found in this station is likely due to the other covarying factors discussed above, caused by the location of the CaTS station and its proximity to riverine influence. Figure 1.9.b shows the cross correlation plot for the Western Atlantic station. The highest correlation ($r = 0.5$) was observed at a time lag of 4. In this analysis 1 time lag is equal to 1 week, therefore four weeks after observing a peak in AOT a peak in Chl_a was observed. Results suggest that at the Western Atlantic station, Chl_a takes approximately one month to react to an input of atmospheric African dust. The weakest correlation between AOT and Chl_a ($r = 0.24$) was found for Atlantic, North of PR station (Figure 1.9.c). The peak in Chl_a concentration was observed at approximately 3 months after the peak on aerosol input, proving little relationship between both parameters. Even though, AOT values had seasonality similar to the other two stations, Chl_a showed little seasonality and extremely low values.

Results obtained at the Western Atlantic, situated directly at the path of the African dust storms, were the most reliable. The high correlation between the time series at a time lag of 4 weeks indicates a time delay in the system. The time lag between atmospheric dust input and chlorophyll concentration might be due to the time required for dust deposition, iron dissolution and iron assimilation by the phytoplankton species present in the region. For example, the transformations from ferric ion (Fe^{3+}) to a more bio-available form (Fe^{2+}) is

carried out mainly by photo-reduction and depends on the time the dust particles spend in contact with the atmosphere and in surface waters. Experiments describing the dissolution processes of iron in seawater exhibit an increase in the dissolved iron concentration after 7 days of adding dust particles (Bonnet and Guieu, 2004). Also, Fe is highly insoluble under conditions of pH higher than 4 (Jickells et al., 2005). Changes in aerosol pH are caused by wetting and drying cycles that are associated to the time aerosols are exposed to a repeated passage of the particles through clouds (Baker et al., 2006).

Weak correlations at the other stations might be the effect of a variety of external factors. For example, the Atlantic, North of PR station is situated at 20°N, 67°W, connecting to southern waters of the Sargasso Sea. Even with high atmospheric iron input toward this region, chlorophyll concentrations may remain low due to lack of dissolved bio-available iron. Studies have found that atmospheric dust deposition is not the only factor controlling dissolved Fe distribution in surface waters of the Sargasso Sea. Factors such as convective mixing, biological Fe uptake and particle scavenging may have an effect on dissolved Fe concentrations in the mixed layer (Wu and Boyle, 2002). Also, surface stratification conditions have been found to strongly affect concentrations of dissolved Fe in these oligotrophic surface waters (Wu and Luther, 1994).

Other factors may contribute to the difference in ecosystem response to African dust input encountered at each station. Marine phytoplankton depends to a great extent on the physical processes that create the upper ocean environment needed for growth. Diverse physical processes that act upon the surface layer of the ocean affect phytoplankton production. For example, patterns of wind stress influence the delivery of nutrients, causing major differences in biomass and community structures (Gargett and Marra, 2002). Also,

upper ocean processes such as wind induce waves and circulations are important to the dynamics of the mixed layer, having pronounced effects on the phytoplankton's environment (Yamazaki et al., 2002). It has been observed that both, the rate of emergence and the duration of a specific physical event, may affect phytoplankton's biomass and production in a given community (Robinson et al., 2002). To fully explain the variability encountered at the three stations would require further studies on this complex relationship between oceanic physical processes and the biology of the phytoplankton population at each station.

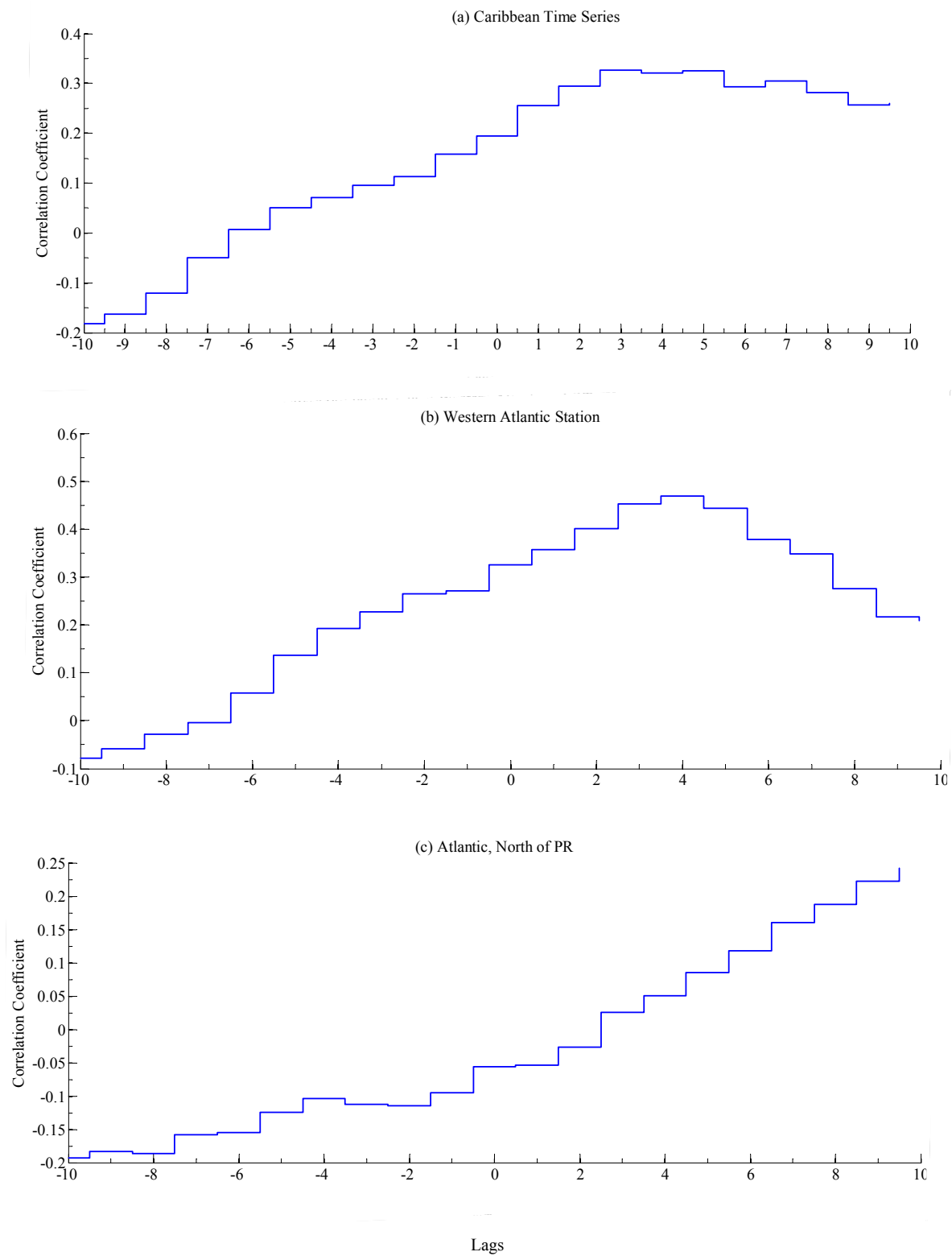


Figure 1.9 Cross-correlation plots for AOT and Chl_a for the (a) CaTS, (b) Western Atlantic and (c) Atlantic, North of PR. A lag represents the number of time steps by which both time series are shifted relative to each other (1 time lag equals 1 week).

Finally, Fe supply by atmospheric mineral dust serves as an important source of fertilization for oceanic photosynthesis. However, light attenuation by scattering and absorption of atmospheric dust particles might affect phytoplankton's photosynthesis. Measurements of the photosynthetically active radiation (PAR) and ultraviolet spectral irradiance at 305 nm were compared with aerosol optical thickness (AOT- 870) to observe light attenuation by atmospheric aerosols. The study was carried out for the summer of 2008 (May-August) at Isla Magueyes field station (17.97°N, 67.04°W) in southwestern Puerto Rico. The summer of 2008 was examined because AERONET level 2 data were available for this station and summer is when maximum Saharan dust loading occurs over this region. A Ground-based Ultraviolet Radiometer system (GUV-511) from Biospherical Instruments Inc. was used to measure PAR and UV (305 nm) while AOT data (Level 2.0, Quality Assured) were obtained from the Aerosol Robotic Network (AERONET). Periods when signatures from clouds were present were discarded and only data collected in cloud-free days were used in the analyses.

Comparisons between PAR and AOT (870) showed no relationships for the studied period (Figures 1.10 and 1.11). For maximum values of AOT, the percent decrease in PAR was about 0.7%. It appears that dust events reaching Puerto Rico were not of sufficient magnitude to cause significant attenuation of PAR during the summer of 2008 (AOT > 0.5). Studies on the effects of dust on light attenuation over West Africa revealed that dust influences oceanic surface available light due to attenuation by AOT values larger than 0.6–0.7 (Mallet et al., 2009). It should be noted that high dust loading could produce a significant effect on PAR and therefore affect primary productivity in certain regions of the ocean. However, this study implies that the amount of desert dust reaching Puerto Rico is not

sufficient to significantly reduce incident PAR and be a forcing agent on regional primary production.

However, when AOT was compared to UV (305), a marked decrease in UV was observed (9%). A strong inverse relationship ($R = -0.502$) between AOT (870) and UV (305) was established for the studied period (Figures 1.12 and 1.13). During summer, dust events reaching the Eastern Caribbean are more frequent and mineral aerosols are abundant in the atmosphere. Mineral particles absorb shortwave solar radiation and are strongly UV absorbing (Dickerson et al., 1997). Kaskaoutisa et al. (2008) showed that low UV values over Greece were directly influenced by an intense Sahara dust load due to strong attenuation of the UV irradiance by the absorbing efficiency of dust particles. Also, Di Sarra, et al. (2002) studied the combined effects of ozone and aerosol in the Mediterranean during May and June 1999, and found a marked dependence of the UV irradiance on the aerosol optical depth influence by dust transported from the Sahara. Even at relatively low AOT values, our results show that desert dust may significantly affect the attenuation of UV radiation through the atmosphere. In regions affected by seasonal desert dust loading, the effect on UV irradiance may be of considerable importance. Solar ultraviolet radiation (UV-B, 280-320 nm and UV-A, 320-400 nm) has been considered a harmful component of sunlight, causing a variety of biological effects within the oceanic euphotic zone. Studies have shown that phytoplankton photosynthesis can be severely inhibited by incident levels of UV radiation at sea surface (Cullen and Neale, 1993). It has been observed that UV is an important ecological factor in aquatic ecosystems and that both UV-A and UV-B are deleterious to some species of phytoplankton (Jokiel and York, 1984). Therefore, reduction in UV by atmospheric dust might have beneficiary effects on biological oceanic production in the studied region.

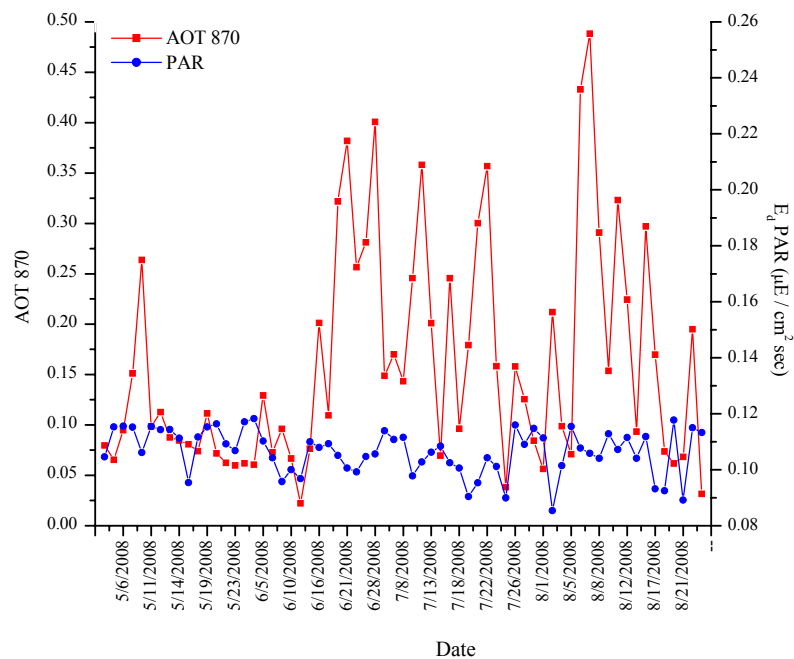


Figure 1.10 Aerosol optical thickness (870) and PAR during May-August 2008 at Isla Magueyes field station.

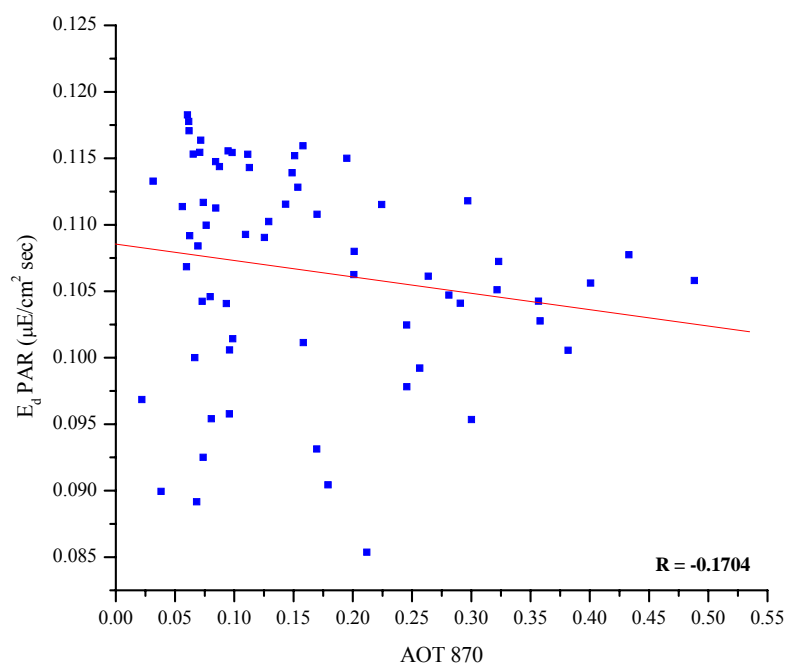


Figure 1.11 Linear fit AOT (870) and PAR during May-August 2008 at Isla Magueyes field station.

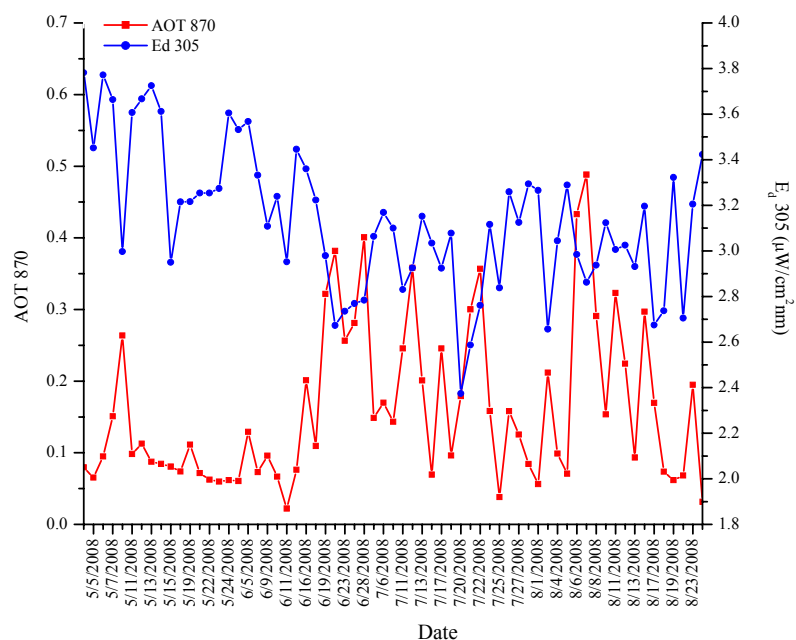


Figure 1.12 Aerosol optical thickness (870) and UV (305) during May-August 2008 at Isla Magueyes field station.

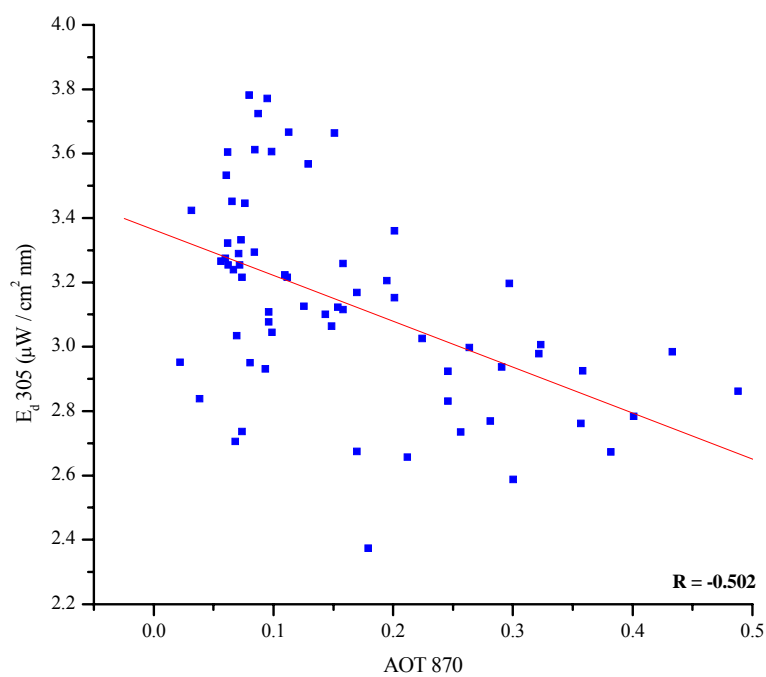


Figure 1.13 Linear fit AOT (870) and UV (305) during May-August 2008 at Isla Magueyes field station.

1.4 Conclusions

Global dust transport and its effects on phytoplankton communities is a major concern in understanding global environmental change. Long term records of atmospheric aerosols and chlorophyll pigment concentrations were evaluated during this study to help describe the effects of iron input in the biogeochemistry of the ocean. A seasonal pattern was encountered for both variables corresponding to the strong seasonal variation in the occurrence of African dust storms. The frequency of the periodic variations in the data indicates that the Tropical North Atlantic Ocean is exposed to cyclic annual dust events. Aerosol optical thickness concentrations recorded during the study are representative of the year-to-year variability of dust export over this region. Maximum mineral dust transport occurs each summer and minimal dust concentrations are present during the winter.

A connection between aerosol load and phytoplankton growth was observed. Elevated aerosol signals were followed by an increase in phytoplankton biomass. In the Western Atlantic Station there is a time delay of 1 month between AOT peak and increase in Chl_a, which might be due to the time required for iron deposition, dissolution and assimilation. Results show evidence for a coupling between satellite derived AOT and Chl_a concentration, supporting the hypothesis that episodic atmospheric delivery of iron stimulates phytoplankton growth in this region. Photosynthetic organisms in the ocean's surface use iron to increase their primary production, which in turn may result in enhanced removal of carbon dioxide from the atmosphere.

This research contributes to the understanding of desert dust storms and its effects on the primary productivity of the ocean. African dust clouds serve as a periodic source of nutrients for primary producers in nutrient depleted oceanic waters. The biogeochemistry of the

Tropical North Atlantic Ocean is therefore influenced by the seasonality of atmospheric dust input, which in turn may have important effects on primary production and climate change.

2. Spectral and Trace Element Analysis of African Soils, Saharan Dust Collected at Sea and Filtered Air Samples for Determination of Iron Content in Mineral Dust

2.1 Introduction

The importance of iron limitation on phytoplankton growth has been evaluated for several decades. The *Iron Hypothesis* developed by John Martin (1994) suggests that Fe availability affects primary production in oligotrophic waters of the ocean. According to Martin (1994) adding Fe to oceanic waters would increase plankton growth by a considerable amount. The *Iron Hypothesis* was tested on the open ocean in an attempt to prove significant blooming of phytoplankton after Fe fertilization of the ocean's surface. This in turn would cause the absorption of carbon dioxide dissolved in the water, drawing the gas out of the atmosphere. In his experiments, Martin, observed that phytoplankton samples with supplemented Fe grew after just a few days. In the presence of Fe, phytoplankton produced biomass at enhanced rates compared to Fe depleted waters, resulting in higher chlorophyll concentrations. Increasing iron content in Fe deficient oceanic regions stimulates phytoplankton growth, increasing the productivity of the area and influencing atmospheric CO₂.

The majority of work on the influence of atmospheric Fe in oceanic fertilization has been carried out on desert soils or aerosols, since mineral dust generated in deserts constitutes the largest source of Fe to the ocean (Baker and Jickells, 2006). Desert mineral dust is transported through the atmosphere supplying Fe to oligotrophic regions of the ocean (Prospero et al., 2002). High dust deposition mitigates Fe limitation increasing oceanic nitrogen fixation and primary production (Moore et al., 2006). Iron availability is a

significant control on oceanic nitrogen fixation, primarily because the enzyme responsible contains large amounts of Fe. Shortage of fixed nitrogen limits phytoplankton's growth and therefore the uptake of carbon dioxide through photosynthesis (Moore et al., 2009). Photosynthetic organisms require nitrogen in the form of nitrate (NO_3^-) or ammonium (NH_4^+) and nitrogen fixation by diazotrophic microbes, such as the blue-green algae *Trichodesmium spp.*, provides a source of usable nitrogen for photosynthesis. In the North Atlantic Ocean, *Trichodesmium* is the principal component of the phytoplankton and N_2 fixation by this organism is a major source of new nitrogen in the region (Capone et al., 2005). An increase in primary productivity due to N_2 fixation increases oceanic sequestration of carbon and may have a significant effect on global climate (Kustka et al., 2002).

Various scientists in different regions of the world have evaluated the effects of aeolian mineral Fe on marine phytoplankton's growth (Martin et al., 1991; Prospero et al., 2001; Kustka et al., 2002; Bonnet and Guieu, 2004; Jickells et al., 2005; Moore et al., 2006). For example, enhanced biological productivity has been observed in the South Indian Ocean, identified as a carbon sink region. The aerosol plume leaving South Africa toward this region may be responsible for Fe fertilization and consequent phytoplankton production (Piketh et al., 2000). Also, on the West Florida shelf, delivery of Fe by Saharan dust has been thought to be responsible for *Trichodesmium spp.* blooms during the summer (Lenes et al., 2001).

Studies of mineral aerosols are important to understand the relationship between atmospheric desert dust and the ocean's biogeochemistry and ecology. In the North Atlantic Ocean, phytoplankton Fe requirements might be supplied by deposition of atmospheric dust, swept into the air over Africa and transported across the Atlantic Ocean. Aeolian desert mineral particulates travel westwards to the Atlantic and Caribbean region via the Sahara–

Sahel Dust Corridor, a zone lying between latitudes 12 °N and 28 °N and running 4000 km west of North Africa (Moreno et al., 2006). Mineral aerosols from these desert regions portray colors in the red, brown and yellow tones, derived mainly from Fe oxides of desert terrain (White et al., 2006). Iron oxides are a major component of desert dust, which contain hematite (Fe_2O_3) as the main form of mineral Fe (Fan Song-Miao et al., 2006). Hematite and other Fe oxides, such as goethite ($\text{Fe}^{3+} \text{O} (\text{OH})$), impart a characteristic color to aeolian sediments, affecting their optical properties (Shen et al., 2006). Studies have shown that both hematite and goethite are strong coloring agents and dominate the spectral signal even in complex matrix containing a variety of minerals (Deaton and Balsam, 1991). When hematite is the main iron oxide, a red color is observed, when goethite dominates, yellow is the major color. This is due to the ion Fe^{3+} contained in both oxides and to the charge transfer between Fe^{3+} and its ligands O^{2-} or OH^- (Elias et al., 2006). Color can therefore serve as an estimate of minerals and iron oxide content on dust aerosols.

Visible reflectance spectroscopy (VRS) may be used to investigate the reflectance characteristics of soil particles and aerosol dust. The spectral signatures of soils are characterized by their reflectance, or absorbance, as a function of wavelength (Brown et al., 2006). The spectral composition and intensity of the reflected energy is related to the mineralogical properties of the soil (Huete and Escadafal, 1991) and allows the recognition of different types based on how they reflect light across a broad wavelength range. By comparing the absorption bands of an unknown material to the absorption bands of known minerals (such as hematite and goethite) we can determine the mineral content of the unknown. Reflectance spectroscopy can be used to determine the presence of Fe oxides in aerosol dust since they have a distinctive red hue and the amount of red in the reflectance

spectrum can be correlated to Fe in the sample (White et al., 2006). The first-derivative of the reflectance curve is then used to identify characteristic peaks of minerals such as hematite and goethite. Studies have shown a relationship between Fe content and the first derivative peaks of the reflectance spectra of minerals providing a tool for making real-time estimates of Fe (Arimoto et al., 2002). Peaks at approximately 565 nm (ranging from 555 to 580 nm) in the first derivative values of the spectrum indicate the presence of the Fe oxide hematite, while goethite has two distinctive peaks at 535 nm and at 435 nm. The height of the first-derivative peak near 565 nm has been reported to be sensitive to hematite and is a function of both hematite concentration and mineral composition of the matrix containing hematite (Torrent and Barron, 2003).

Elemental analysis is important to further confirm and quantify the presence of Fe and other trace metals in soil, dust and air samples. Since 1980, inductively coupled plasma mass spectrometry (ICP-MS) has emerged as a useful technique for the analysis of soil due to its multi-element capability, high detection power and low sample consumption (Falciani et al., 2000). The method combines sample introduction and analysis of ICP technology with the accurate and low detection limits of a mass spectrometer. Due to its high sensitivity, sample amount needed for the analysis can be very small.

Atmospheric dust traveling from North Africa toward the Atlantic Ocean consists typically of mineral mixtures derived from different geological sources. Desert sands commonly retain a strong signature of their source area at significant distances from their origin, so the parent material has an important influence on atmospheric dust (Castillo et al., 2008). The main objective of this study is to investigate the presence of Fe in aeolian desert mineral particulates at their source (African soils), during their atmospheric transport across

the Atlantic Ocean (Saharan dust collected at sea) and finally, to the fraction reaching remote land areas (filtered air samples collected in southwestern Puerto Rico). Spectral reflectance characteristics of samples (African soils and Saharan dust collected at sea) were examined using reflectance spectra and first derivative analysis for signals from iron-bearing minerals. These samples, as well as the filtered air samples were then analyzed for trace metals by ICP-MS using a microwave digestion procedure (EPA, 3051-A). The study focused on Fe and Al, two elements typically found in dust originating in desert regions. Chemical composition of African dust in previous studies has revealed that both, Fe and Al, are the main components (Jiménez-Vélez et al., 2009). Trace element ratios (Fe/Al) of samples, was also calculated to characterize Saharan dust and to observe a common regional source of dust formation.

2.2 Materials and Methods

Desert surface soil samples were collected from Nigeria, Sudan, Mali and Morocco; four North African Countries with different geological settings (Figure 2.1). Saharan dust air samples were collected at sea during the Trans-Atlantic Saharan Dust Aerosol and Ocean Science Expedition (AEROSE 2004), aboard the NOAA Ship Ronald H. Brown (Figure 2.2 and 2.3). Samples were collected on March 6, 2004 (Figure 2.3.a) when the ship encountered an unusually massive plume of Saharan dust midway across the Atlantic Ocean (Morris et al., 2006) and after the dust storm on March 14, 2004 (Figure 2.3.b). The cruise tracks coincided with one of the biggest dust storms for this season (Figure 2.4).



Figure 2.1 Soil samples collected from Nigeria, Sudan, Mali and Morocco.

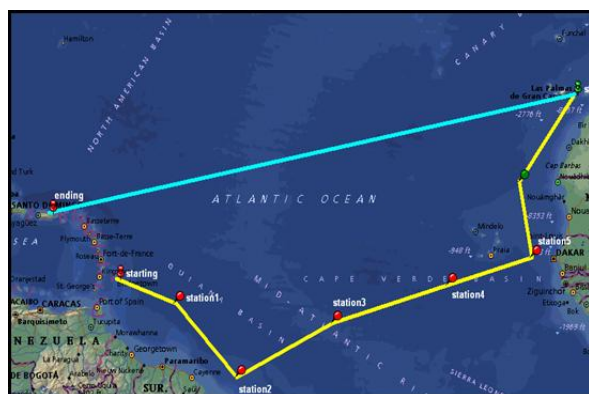


Figure 2.2 Trans-Atlantic Saharan Dust Aerosol and Ocean Science Expedition (AEROSE 2004) cruise tracks.



(a) March 6, 2004 (b) March 14, 2004

Figure 2.3 Saharan dust collected at sea, AEROSE 2004.

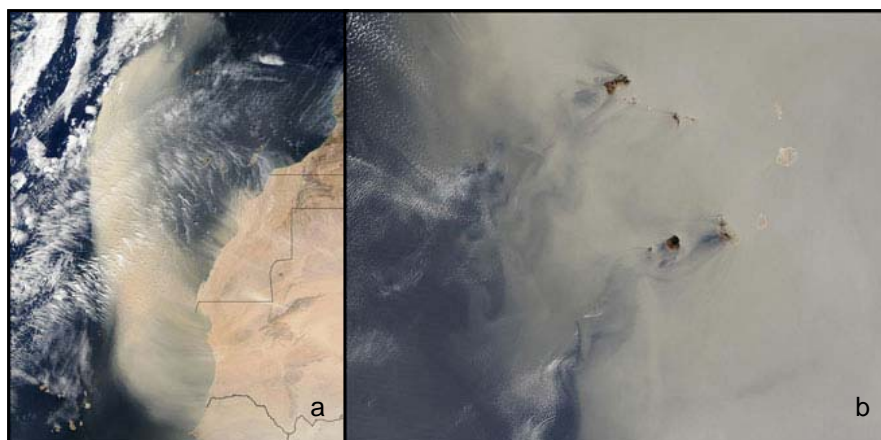


Figure 2.4 MODIS Terra satellite images for March 2004, showing large Saharan dust storms leaving Africa (a) and moving over the Atlantic Ocean to cover Cape Verde islands (b).

A Fine Particulate Chemical Speciation Air Sampler (RAAS 2.5- 400) from Thermo Andersen Instruments Inc. was used to collect PM_{2.5} air samples (Figure 2.5) at Isla Magueyes field station (17.97° N, 67.04° W) in southwestern Puerto Rico. The Thermo Andersen Reference Ambient Air Sampler (RAAS) 2.5-200 (Figure 2.6) was used to collect filter samples for chemical and gravimetric analysis of PM_{2.5} ambient air particulate matter. The RAAS sampler specification is contained in 40 CFR Part 50 Appendix L. It operates at a fixed flow rate of 16. 67 liters per minute (one cubic meter per hour) and uses a specified inlet, tubing, secondary size selective impactor (WINS impactor), and filter holder. The air inlet removes particles larger than 10 µm and the WINS impactor excludes particles larger than 2.5 µm. The system pulls ambient air through a protective inlet preventing water and wind distortions while sampling and can be operated under a wide range of environmental conditions. The particulate was collected on a 47mm filter (PTFE) during 24-hour sampling periods.

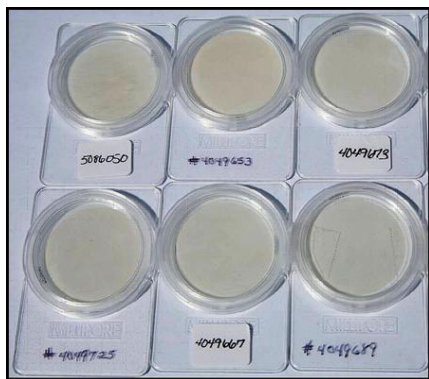


Figure 2.5 Air samples collected at Magueyes Field Station.



Figure 2.6 The Thermo Andersen RAAS 2.5-200 air sampler
www.uprm.edu/bio-optics/aerosols.html

Dust events reaching the Eastern Caribbean are more frequent during summer months, so our samples were collected on Whatman PTFE PM_{2.5} filters (2µm) during the summer of 2007. Filters inspection, pre-conditioning (20-23°C and mean humidity 30-40%), pre-weighting and post-conditioning and weighting were conducted at the Environmental Quality Board (San Juan, PR). Filters were placed on a clean Millipore Petrislide and stored until transferred to the laboratory for a microwave acid digestion procedure followed by ICP-MS to measure trace metal content.

Reflectance spectra were used to relate samples of African soil and Saharan dust collected at sea qualitatively with two standards, hematite and goethite (Figure 2.7), based on the known relationship between color and Fe oxides. The spectra of the samples were measured outdoors with a spectroradiometer (GER 1500) from 400 to 800 nm to determine the presence of Fe bearing minerals. The GER 1500 is a field portable spectroradiometer (from Geophysical and Environmental Research Corporation) used for acquiring data covering the UV, Visible, and NIR wavelengths (350-1050 nm). It is design for remote sensing studies without the need of computers and cables during data acquisition, which can be accomplished by hand-held or tripod operation. Simple menu-driven programs control the

set-up, acquisition, and data manipulation functions. Data is stored in ASCII format for easy transfer to other software programs.

First-derivatives of the percent reflectance curves were used to identify more clearly characteristic peaks of hematite and goethite. These peaks were used to observe presence of Fe oxides in African soils and Saharan dust collected at sea, since the color or the shape of the curve is indicative of the iron content. Data processing was limited to the visible spectral region, the most sensitive to Fe oxide minerals.



Figure 2.7 Standard samples: hematite (a) and goethite (b).

Mass and elemental concentration on samples were analyzed by ICP-MS (Agilent 7500ce) following the EPA method 200.8 for quantification of trace elements. The method is designed for the determination of dissolved elements in ground waters, surface waters and drinking water. It may also be used for measurement of total element concentrations in soils samples, where a digestion/extraction is required prior to analysis (when elements are not in solution). The Agilent 7500ce ICP-MS is designed for analyzing environmental, clinical and other high matrix samples. It provides reliable detection limits for trace elements in wastewater, seawater, soils, foods and biological samples and incorporates an Octopole Reaction System (ORS) for interference removal in high matrix samples. The ORS is used for routine trace analysis of complex, variable and unknown samples. It removes interferences independently of the analyte of the sample matrix. Unknown samples can therefore be analyzed without requiring matrix-specific or element-specific optimization. The analytical performance of the ICP-MS depends on the energies imparted to ions in the plasma, which can have a significant effect on the efficiency of the sampling of those ions and their subsequent analysis by the mass spectrometer. The ion energies are a direct consequence of the electromagnetic characteristics of the plasma, which in turn, are determined by the plasma induction coil and its associated radio frequency (RF) supply.

In our study, 0.25 g of African soils and Saharan dust collected at sea was weighed before processing and then solubilized by gentle refluxing with nitric acid (10 ml). Soil and dust sample were then digested in a MARS-X Microwave Digestion System (CEM), along with the filtered air samples. The microwave accelerated reaction system is designed for laboratory extraction of organic compounds from solid matrices. The process involves heating solid sample-solvent mixtures with microwave energy in a closed system and

subsequent partitioning of compounds from the sample to the solvent. Heating is achieved by non-ionizing radiation energy that causes migration of ions and rotation of molecules with dipole moments, without causing changes in molecular structure. During the extraction process, exposure to the electric component of the microwave field causes the alignment of polar solvent-sample molecules. Elevated temperatures are achieved by speed of microwave heating and sealed vessel technologies. This combination of high temperature and rapid heating in a closed-vessel system increases the extraction efficiency and reduces the extraction time.

Samples were heated at 175 °C for 10 minutes during the microwave extraction. After cooling, the samples were made up to volume (200 ml), mixed and centrifuged. The material in solution was then introduced into radio-frequency plasma by pneumatic nebulization, a method used to generate a fine aerosol of the sample so it can be efficiently ionized in the plasma discharge. Once the sample passes through the nebulizer and it is partially desolvated, removing any remaining solvent. The hot plasma then causes sample atomization, or reduction of sample into atoms, followed by ionization, where ions are produced. Finally, ions were extracted from the plasma through a differentially pumped vacuum interface and separated on the basis of their mass to-charge ratio. Blank filters were processed simultaneously with samples and trace elements values in blanks were subtracted from those obtained for each sample filter. Iron and aluminum element concentration was calculated from the ICP-MS measured concentration divided by the total sample weight.

2.3 Results and Discussion

Spectral Analysis

Reflectance curves of African soils and Saharan dust sample collected at sea are illustrated in Figures 2.8.a and 2.9.a respectively. Both samples present characteristic spectral properties of the standards, hematite and goethite (Figure 2.10.a) and agree with the fact that colored Fe oxides absorb strongly in the blue spectral regions and reflect in the red and near-infrared (NIR) regions. Our observations coincide with published reflectance spectra for hematite and goethite, showing high absorption between 400 and 550 nm (Kosmas et al., 1986). Calculation of the first derivative of the reflectance curves was used to identify more clearly the presence of Fe oxides in African soils and Saharan dust samples collected at sea (Figure 2.8.b and 2.9.b) with respect to our standards (Figure 2.10.b). The peaks of the first derivative for our samples exhibit characteristic spectral properties of Fe oxides described in previous literature (Deaton and Balsam, 1991; Arimoto et al., 2002; Shen et al., 2006; White et al., 2006). First derivatives plots show distinctive peaks ranging from 555 to 580 nm, with the majority of the peaks lying near 565 nm, a spectral range typical of hematite. Smaller peaks near 435 nm are representative of samples containing goethite. Subtle differences in reflectance curves and first derivative values between samples may be attributed to factors that may affect the color including particle size and shape, crystal defects, adsorbed impurities, and the degree of particle packing (Torrent and Barron, 2002).

Previous studies have confirmed that color variability is a mineral intrinsic property, and therefore can be used to identify hematite and goethite with high reliability (Scheinost and Schwertmann, 1999). Also, it has been stated that observed optical properties of the aerosols may be related to the chemical composition and concentration of iron in mineral dust

(Arimoto et al., 2002). First derivative values at wavelengths characteristics of hematite and goethite indicate presence of these iron-bearing minerals in both African soils and Saharan dust samples. The results show that iron oxides are important in determining soil and dust reflectance properties and further demonstrate a relationship between Fe concentrations and the first derivative peaks for hematite and goethite. Visible reflectance spectroscopy is proven to be useful for identifying Fe content in mineral aerosols relative to the color of the samples.

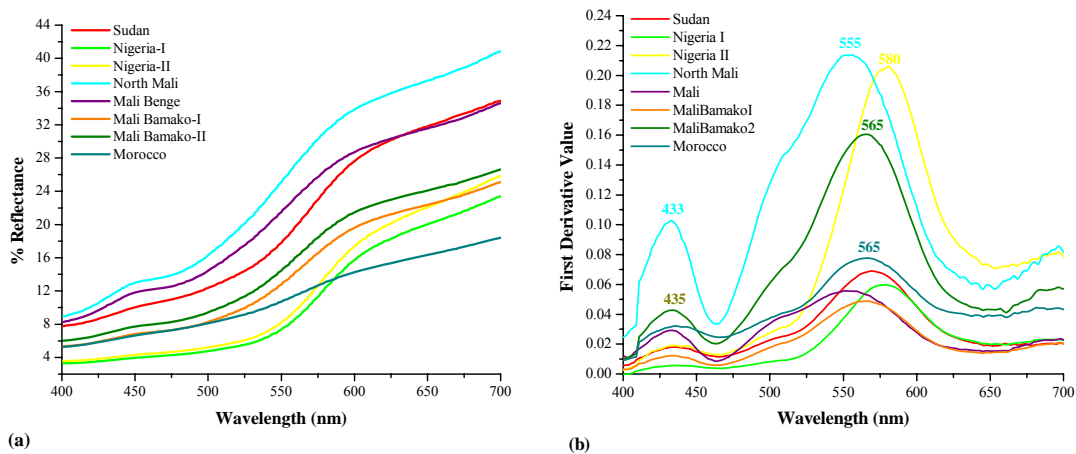


Figure 2.8 Percent reflectance spectra (a) and first derivative plots (b) of soil samples collected in North Africa.

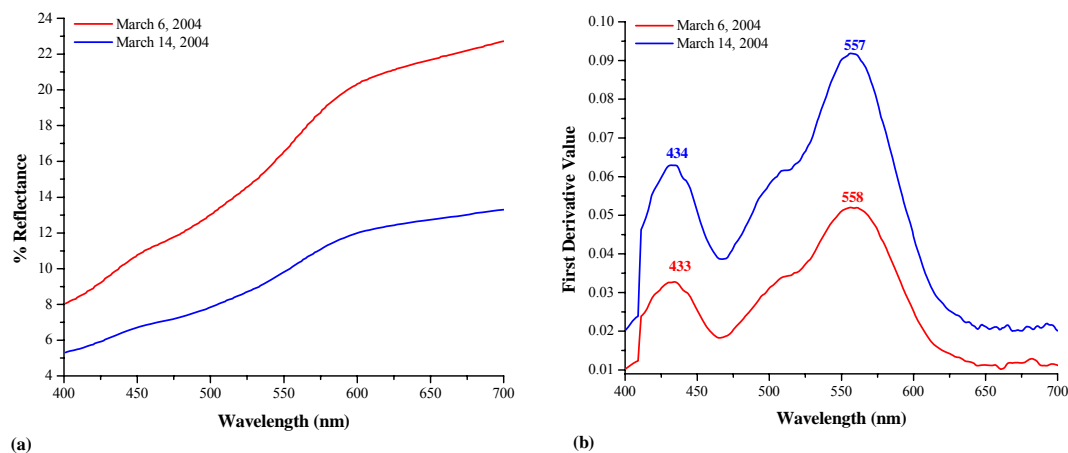


Figure 2.9 Percent reflectance spectra (a) and first derivative plots (b) of dust samples collected at sea, during AEROSOL 2004.

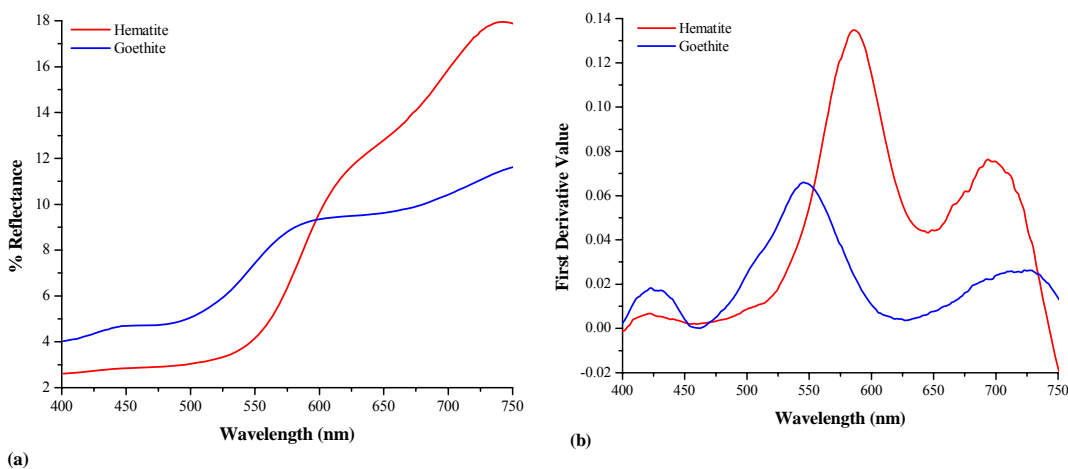


Figure 2.10 Percent reflectance spectra (a) and first derivative plot (b) for hematite and goethite standards.

Iron and Aluminum Elemental Analysis

Percent Fe and Al were calculated for soil samples collected at various sites in North Africa (Figure 2.11). Different geological settings between soil samples may be responsible for the high variability observed in the values of percent Fe, ranging from 0.03 in Sudan to approximately 0.7 in Mali Bamako (I). Percent Al varied from 0.02 in Sudan to 1.04 in Mali Bamako (I). Previous studies show that concentrations of major elements, such as Fe and Al are more variable in soil samples collected in source regions than in the transported Saharan dusts (Guieu et al., 2002). This can be further observed in results from dust collected during AEROSE, which showed a higher level of homogeneity for both, percent Fe and Al (Figure 2.12). Consistency of the Fe/Al mass ratios in both samples (0.75 for March 6 and 0.71 for March 14) suggests a common regional source of dust formation. Previous studies of aerosols over the North Atlantic Ocean have observed Fe/Al mass ratios of 0.72 ± 0.064 (Bates et al., 2000), which are consistent with our findings.

Filtered air samples collected at Magueyes Field Station also resulted in high variability in percent Fe and Al (Figure 2.13). Iron ranged from 1.09 to 2.16, while Al ranged from 1.42 to 2.38. Differences between samples were also observed in the calculated Fe/Al ratios, ranging from 0.61 to 1.16 with an average value of 0.74. In general, Fe/Al ratios of Saharan mineral dust transported toward the Caribbean region showed a higher variability than the samples collected at sea during AEROSE. This difference is probably related to alterations in the chemical composition and PM size distributions during transport by processes that will tend to mix dust from different source regions. Dusts derived from different geological sources, and the size distribution of the particles will tend to change with transport and time (Castillo et al., 2008). Also, differences in Fe/Al ratios may be attributed to difficulties in

measuring Al with current ICP-MS procedures and instrumentation (Prospero and Landing, 2009).

Statistical analysis shows very high variability in percent Fe and Al (Table 1.2) between all our samples. Maximum values of both, Fe and Al were observed for the filtered air samples, while African soils resulted in minimum values. From Figure 2.14 it is clear that as particles become smaller, (from African soils to filtered air samples) the percent Fe and Al in the samples increases. As African dust travels through the atmosphere, their bulk chemical composition and PM size distributions are altered. Physical and chemical processes on the parental materials during transport will have an effect on particle size ranges and accessory mineral, which in turn controls the chemistry of trace element. Previous studies have shown that Fe and Al are favored in samples of finer materials (Castillo et al., 2008).

Trace element analysis shows evidence of the presence of Fe in samples from desert mineral soils, from the origin of the dust formation through their atmospheric transport across the Tropical North Atlantic Ocean. Also, this study further confirms that the percent trace elements are relatively higher in the finer particle size samples transported away from the desert.

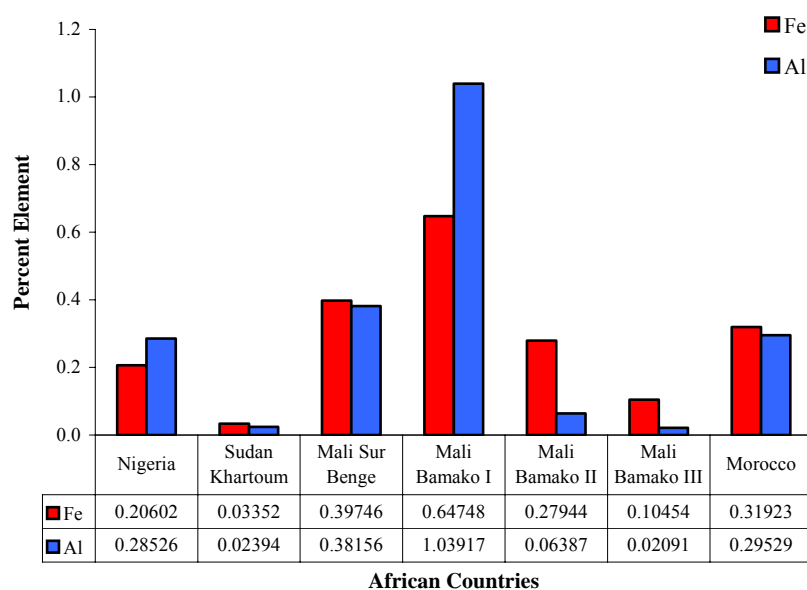


Figure 2.11 Percent Fe and Al in soil samples collected from different North African countries.

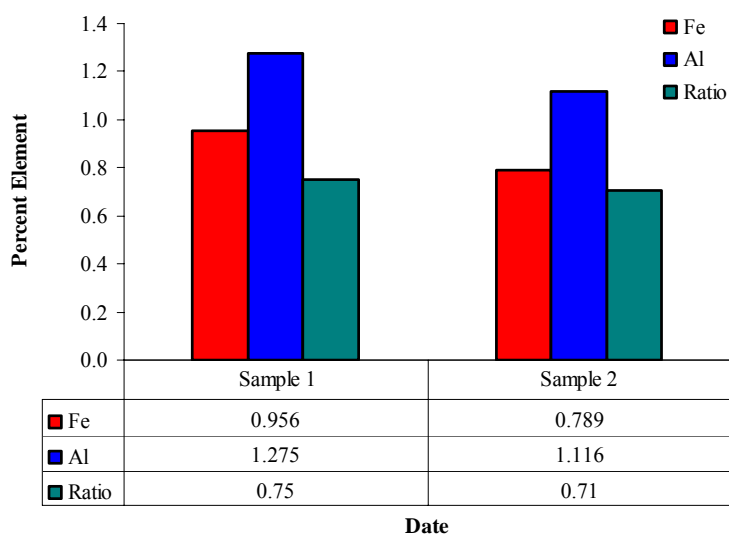


Figure 2.12 Percent of Fe and Al in Saharan dust samples collected at sea during AEROSE 2004. Sample 1 was collected during March 6, 2004 and sample 2 during March 14, 2004.

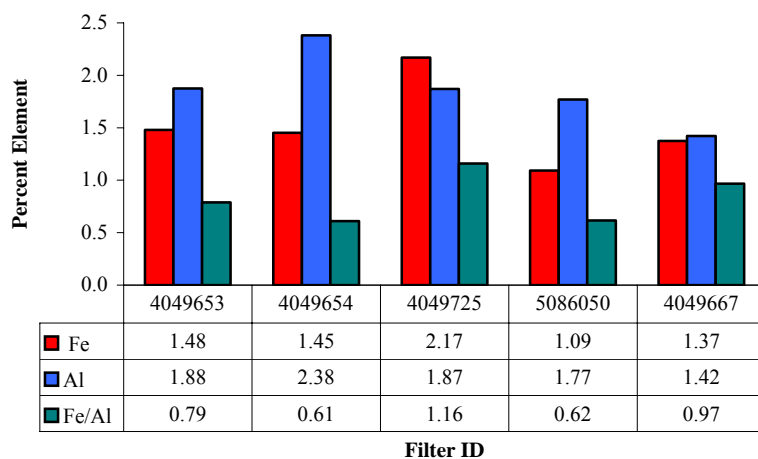


Figure 2.13 Percent Fe and Al in filtered air samples collected at Puerto Rico, Magueyes Field Station.

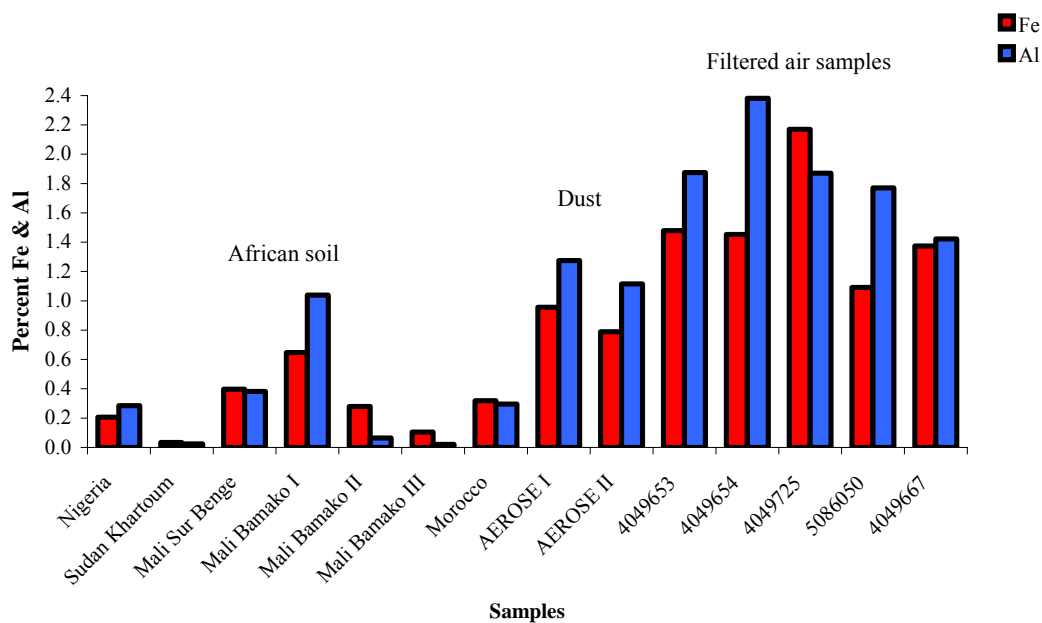


Figure 2.14 Percent Fe in African soil, Saharan dust and filtered air samples.

Table 2.1 Statistics: All Samples

Statistics	Fe	Al
Maximum	2.17	2.38
Minimum	0.03	0.02
Average	0.81	0.99
Std Dev.	0.64	0.81

2.4 Conclusions

Atmospheric dust transported from desert regions toward the North Atlantic Ocean is an important pathway for dispersion of nutrients and trace metals from continents to the oceans. Mineral particles traveling westwards from Africa to the Atlantic region via the Sahara–Sahel Dust Corridor portray colors in the red, brown and yellow tones, derived mainly from Fe oxides of desert terrain. This study demonstrate that visible reflectance spectroscopy is a useful technique for qualifying Fe content in desert mineral aerosols relative to changes in color of the samples. Iron oxides in atmospheric desert particles exhibited a characteristic color that can be related to Fe content. The first derivative of the reflectance curves provided a tool to correlate distinctive peaks with iron bearing minerals. Visible reflectance spectroscopy was proven to be a fast, non-destructive technique to identify Fe oxides in soil and dust samples and may be used to overcome limitations of other techniques for identifying trace amounts of iron oxides. Furthermore, first derivative curves resulted in excellent qualitative indicators of iron bearing minerals in our samples

The trace element analysis by inductively coupled plasma mass spectrometry (ICP-MS) provided further confirmation of Fe content in African soils, Saharan dust and filtered air samples. Iron and Aluminum content of the transported Saharan dust was more homogeneous than the composition of individual African soils and the filtered air samples. Higher variability found in air samples collected far away from the source is probably due to particle mixing and alterations in chemical composition and PM size distributions, which tend to change with distance and transport time. A higher level of homogeneity for both, percent Fe and Al, was observed for dust collected during AEROSE and Fe/Al ratios suggested a common regional source of dust formation. Our results show that as African dust travels

through the atmosphere and PM size become smaller, percent Fe and Al increase. Iron was therefore favored in the filtered air samples collected at greater distance from the source. Our findings confirm that percent trace elements are higher in the finer particles transported away from the desert and may supply phytoplankton's Fe requirements for oceanic nitrogen fixation at great distances from their geological formation.

3. Satellite and Ground-based Aerosol Optical Thickness and Chlorophyll Concentration in the Tropical North Atlantic Ocean (March, 2004)

3.1 Introduction

Atmospheric aerosols originating in arid and semi arid regions of the world, such as the Sahara desert, are responsible for a variety of climate, health, and environmental impacts, both on global and regional scale (Morris et al., 2006). Atmospheric aerosols play an important role in climate change acting on the earth's energy budget. They directly affect climate by reflecting and absorbing solar radiation and indirectly by modifying cloud optical properties, generation and lifetime (Wang et al., 1999). Dust deposited in the Atlantic Ocean also provides key nutrients such as iron to oceanic phytoplankton (Kaufman et al., 2002). Nutrients supplied by particles traveling from the Sahara desert to oligotrophic regions of the ocean, have an effect on the biogeochemical cycle and primary productivity of the area (Prospero et al., 1981; Claustre et al., 2002). Studying the interaction between Fe input and phytoplankton ecosystem dynamics is important since deposition of Fe from mineral aerosols can impact the carbon cycle (Mahowald et al., 2005). Aerosol optical properties, such as aerosol optical thickness (AOT), are therefore crucial in understanding the effects of atmospheric aerosols in climate forcing and biogeochemical cycling. Aerosol optical thickness measures the radiation extinction at the encounter of aerosol particles in the atmosphere due to aerosol scattering and absorption. It is a measure of the degree to which aerosols prevent the transmission of light. In general, higher AOT values are indicative of higher column aerosol loading and lower visibility (Wang and Sundar, 2003).

To accurately study aerosol distribution and their impacts on the environment requires continuous observations from satellites, ground-based instruments and field experiments (Kaufman et al., 2002). Satellite-based measurements have been proven to provide excellent source of data and have greatly improved the knowledge of the distribution of aerosols in the atmosphere (Myhre et al., 2005). Compared to *in-situ* observations, satellite imagery has large spatial coverage and repeated measurements, providing an important tool to monitor aerosols and their transport (Wang and Sundar, 2003). Recently, the Goddard Earth Sciences Data and Information Services Center created the web-based application GIOVANNI (GES DISC Interactive Online Visualization and ANalysis Infrastructure). Giovanni facilitates visualization and analysis of satellite remotely sensed data sets. It offers different temporal and spatial resolution data, making it possible to investigate regional and global events. Giovanni is comprised of a number of interfaces, which include both atmospheric and oceanographic data (<http://giovanni.gsfc.nasa.gov>). Giovanni's atmospheric data is the result of daily level-3 aerosol parameters including measurements from Terra and MODIS Aqua.

Chlorophyll concentration may also be obtained from Giovanni's Ocean Instances, but in contrast to AOT data, Chl_a is not produced by direct satellite observations. Total chlorophyll is a data product generated by the NASA Ocean Biogeochemical Model (NOBM) based on data assimilation of remotely sensed Chl_a. The NOBM utilizes satellite chlorophyll data in a coupled three-dimensional model that incorporates general circulation, biogeochemical, and radiative components (Gregg, 2008).

However, remotely sensed data are subjected to errors resulting from calibration, atmospheric correction, uncertainties in atmospheric optical state and problems deriving chlorophyll from radiances (Gregg and Conkright, 2001). In order to understand how well

satellite measurements describe atmospheric and oceanographic bio-optical properties, it is important to complement satellite data with ground-based observations. Ground-based AOT measurements are critical to characterize and understand the impacts of Saharan dust in the ocean's biogeochemistry, as aerosols are transported across the North Atlantic Ocean. The Aerosol and Oceanographic Science Expedition (AEROSE) sponsored by the NOAA Center for Atmospheric Sciences (NCAS) was conducted from February 29 to March 26 2004 onboard the NOAA Ship Ronald H. Brown. The expedition provided a unique set of atmospheric and oceanographic measurements, such as AOT and chlorophyll concentration, across the North Atlantic Ocean. The cruise departed from Bridgetown, Barbados, traveling eastward toward Africa, taking a north route toward the Canary Islands and finally returned to San Juan, Puerto Rico (March 26). The cruise tracks coincided with an unusually massive plume of Saharan dust midway across the Atlantic Ocean (Morris et al., 2006). During the expedition an interdisciplinary team of scientists obtained satellite, atmospheric, and oceanographic measurements such as AOT and Chl_a concentration. Ground-based AOT data and surface chlorophyll concentrations were measured daily during AEROSE 2004.

In this study, AOT and chlorophyll satellite observations from Giovanni were compared with ground-based measurements obtained during AEROSE 2004. Giovanni's AOT from MODIS-Aqua (550 nm) was compared with Microtops ground-based AOT at different wavelengths, while *in-situ* Chl_a was compared with Giovanni's NOBM Assimilated Total Chlorophyll product. This study is intended to observe the potential of satellite measurements in describing atmospheric and oceanographic bio-optical properties and to complement satellite data with ground-based observations. Also, monthly Giovanni's AOT and Chl_a products were compared to determine if a relationship between African dust input and Chl_a

concentration can be established using Giovanni's satellite data. Products were retrieved for the Western Atlantic Station defined in Chapter I (19°N, 57°W) from August 2002 to December 2005.

In the last section of this study we examine the variability of dust distribution in relation to the North Atlantic Oscillation (NAO) index. Studies have shown that the NAO index influences the large-scale variability of atmospheric circulation in the Northern hemisphere (Hurrell, 1995). In general, high NAO index yields drier conditions over southern Europe, the Mediterranean Sea and northern Africa, while low NAO years, causes precipitation over the Mediterranean and large areas of North Africa, limiting the intensity of dust uptake and transport (Moulin et al., 1997). The studied period (March, 2004) coincided with one of the biggest dust storms for this season (Figure 3.1). We examined the dust distribution and NAO index for the Western Atlantic Station to observe if the unusual dust event encounter during March 2004 was related to the NAO.

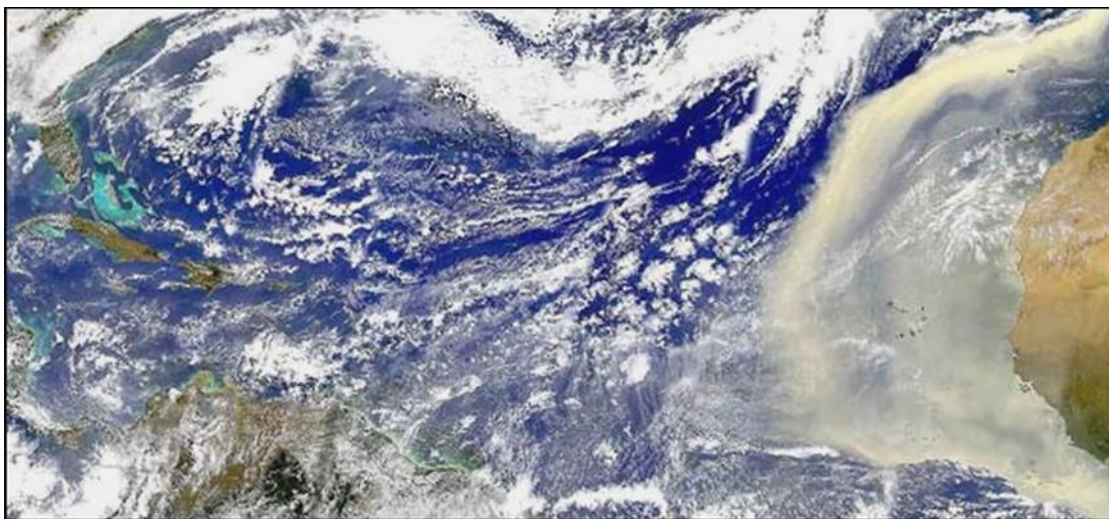


Figure 3.1 MODIS two-day composite true color image showing Saharan dust event leaving North Africa (March 2 -3, 2004).

3.2 Materials and Methods

Shipboard Measurements (AOT and Chlorophyll a)

Aerosol and Chl_a observations were conducted onboard the NOAA Ship Ronald H. Brown between February 29 and March 26, 2004. Onboard ship measurements for AOT and Chl_a were carried out at various dates and locations along the cruise track (Tables 1.3 and 2.3). A Microtops II (Solar Light Co.) handheld sun-photometer was used to measure attenuation of the direct sunlight as it passed through the atmosphere. The Microtops II is a 5-channel sun-photometer for measuring aerosol optical thickness at each of 8 possible standard wavelengths, 340, 380, 440, 500, 675, 870, 936, and 1020 nm, and provides the option to choose up to 5. It has been designed for column measurements of water vapor, ozone and total aerosols. The aperture of the instrument is small so that atmospheric scattering does not influence the light intensity measured. Atmospheric AOT is therefore derived from measurements of the total transmittance (Retalis and Hadjimitsis, 2010). During AEROSE (2004), Microtops II instruments were set to obtain total column aerosol optical depth observations in different bands of the solar spectrum centered at 340, 380, 870 and 1020 nm. These measurements were collected and provided by the Howard University NCAS team.

Daily chlorophyll-a concentrations were obtained from the continuous near surface sampling flow-through system installed on-board the Ronald H. Brown. The system measured automatically chlorophyll- a salinity, temperature and nutrient concentrations.

Table 3.1 Dates and ship position of AOT measurements, AEROSE 2004.

Date	Latitude	Longitude
3/4/2004	6.16	-40.63
3/5/2004	6.17	-40.44
3/6/2004	8.22	-36.28
3/7/2004	9.90	-32.99
3/8/2004	11.37	-28.76
3/9/2004	12.83	-24.61
3/10/2004	14.29	-20.46
3/11/2004	17.85	-19.00
3/12/2004	20.66	-20.81
3/13/2004	23.77	-19.13
3/14/2004	26.70	-16.28
3/17/2004	28.65	-15.44
3/18/2004	28.99	-20.01
3/19/2004	28.56	-25.72
3/21/2004	27.31	-36.99
3/22/2004	25.61	-43.70
3/23/2004	24.18	-49.30
3/24/2004	22.67	-54.43
3/25/2004	20.75	-60.16
3/26/2004	18.79	-65.47

Table 3.2 Dates and ship positions of Chl_a measurements, AEROSE 2004.

Date	Latitude	Longitude
3/1/2004	11.81	-56.02
3/2/2004	9.89	-52.75
3/3/2004	6.81	-49.60
3/4/2004	6.16	-45.53
3/5/2004	6.25	-40.94
3/6/2004	7.72	-37.40
3/7/2004	9.44	-33.96
3/8/2004	11.34	-28.86
3/9/2004	12.49	-25.59
3/10/2004	14.28	-20.71
3/11/2004	16.76	-19.00
3/12/2004	20.52	-20.50
3/13/2004	23.58	-19.31
3/14/2004	26.86	-16.15
3/15/2004	28.14	-15.42
3/17/2004	29.17	-15.50
3/18/2004	28.97	-20.09
3/19/2004	28.43	-26.88
3/20/2004	27.71	-32.65
3/21/2004	26.70	-38.58
3/22/2004	25.57	-43.87
3/23/2004	24.08	-49.66
3/24/2004	22.49	-55.00
3/25/2004	20.49	-60.84
3/26/2004	18.92	-65.12

Satellite Observations

Aerosol optical thickness and chlorophyll concentration data were retrieved from the Giovanni web page (<http://disc.sci.gsfc.nasa.gov/giovanni>). Both products were obtained for each day and ship position corresponding to AEROSE ground-based measurements. The level 3 AOT product (MODIS Aqua-Version 5.1) was retrieved from the daily atmospheric instances at a 1° spatial resolution. The algorithm for remote sensing of atmospheric aerosol

is comprised of two independent algorithms, one for deriving aerosols over land and the second for aerosols over ocean. It is based on a lookup table (LUT) approach, where radiative transfer calculations are pre-computed for several values of the aerosol and surface parameters. Spectral reflectance from the LUT is compared with MODIS-measured spectral reflectance to find the least-square fit (Tanré et al., 1997).

Chlorophyll concentration was obtained from Giovanni's ocean instances. Total Chlorophyll (NOBM) data (expressed in mg/m^3) was used for the analysis. The NOBM is a coupled three-dimensional model that incorporates general circulation, biogeochemical, and radiative components (Gregg, 2008). The model includes influences from ocean circulation and turbulence, irradiance availability, and the interactions among four phytoplankton functional groups (diatoms, chlorophytes, cyanobacteria, and coccolithophores) and nutrients data (nitrate, ammonium, silica, and dissolved iron) (Gregg, 2003). The *Ocean General Circulation Model* is a reduced-gravity representation of circulation fields (Schopf and Lough, 1995), while the biogeochemical processes model includes different phytoplankton functional groups, nutrient groups and detrital pools and the *Ocean-Atmosphere Radiative Model* (Gregg, 2002) provides radiative transfer calculations.

Monthly Giovanni's AOT and Chl_a products were retrieved for the period of August 2002 to December 2005 for the Western Atlantic Station (19 °N, 57 °W). The data was compared to determine if a relationship between African dust input and Chl_a concentration can be established using Giovanni's satellite data.

Finally, Giovanni's monthly AOT (MODIS Aqua) was compared with the NAO index (http://www.cpc.noaa.gov/products/precip/CWlink/pna/nao_index.html) for 2004 and from 2003 to 2007.

3.3 Results and Discussion

Satellite and sun-photometer measurements were used to evaluate aerosol optical thickness data for the North Atlantic Ocean. Aerosol optical thickness was measured at different wavelengths using satellite (Giovanni 550) and ground-based sun-photometer (Figure 3.2). A strong linear relationship ($R^2 = 0.86$) was found between Giovanni AOT 550 and Microtops 870 (two wavelengths typically used for describing atmospheric dust particles) for the studied days and ship positions (Figure 3.3). Even though the spatial and temporal sampling properties of satellite and ground-based measurements are different, there is good agreement between both data sets. These results imply that MODIS AOT data provides accurate information of aerosol loading for the studied area. This was further confirmed with an analysis of variance where no significant differences between ground-based and satellite measurements were observed (Table 3.3). Significant correlations between direct comparison of MODIS and handheld sun-photometer AOT have been published for different regions of the world. For example, Retalis and Hadjimitsis (2010) compared aerosol data retrieved from satellite and sun-photometer at various locations in Cyprus and found strong correlation ($r=0.83$) between both measurements. Also, studies of AOT over the South East Arabian Sea compared MODIS aerosol parameters with ship borne Microtops measurements with correlations between 0.96–0.97 (Aloysius et al., 2009).

Satellite and *in-situ* Chl_a measurements are illustrated in Figure 3.4. High variability was observed between the two data sets with a percent difference of 56%. An analysis of variance also resulted in significant differences between satellite and *in-situ* Chl_a measurements (Table 3.4). Our results indicate that remote sensed data underestimates chlorophyll concentrations for the studied area. Underestimation of satellite Chl_a has been

widely observed in previous studies. For example, studies with the Coastal Zone Color Scanner have resulted in underestimations of global chlorophyll concentrations when compared with *in-situ* measurements in different regions of the ocean (Gregg and Conkright, 2001). Also, research in the Southern Ocean reported SeaWiFS satellite underestimates of Chl_a relative to *in-situ* measurements (Moore et al., 1999). Even so, although Chl_a concentrations from satellite data are much lower than the measured values (especially at high *in-situ* chlorophyll values), there is a good agreement between satellite and *in-situ* measurements (Figure 3.5). The relationship between chlorophyll-a values from ground-based data and Giovanni's product resulted in an R^2 of 0.76. Studies in the Scotia Sea also presented a strong relation between SeaWiFS Chl_a and on board ship data ($R^2 = 0.82$), with the satellite data underestimating the *in-situ* values at high Chl_a concentrations (Holm-Hansen et al., 2004).

Differences between satellite and ground-based measurements may result from many factors. Remotely sensed data are subject to several sources of error such as calibration, atmospheric correction errors, uncertainties in atmospheric optical state (Gregg and Conkright, 2001) nearness to coast, or the presence of other substances and particles that affect the light levels observed by the satellite. Also, discrepancy in spatial scale between *in-situ* samples taken from a few liters of water and satellite estimates based on averaging over a pixel with large dimensions, can affect the results (Holm-Hansen et al., 2004). The spatial resolution of Giovanni's satellite product used for this study is of $1^\circ \times 1^\circ$ ($\sim 110 \text{ km}^2$), compared to a few meters on the ground-based data. This should be considered when comparing both measurements. Underestimation of satellite Chl_a is the result of the distribution of surface chlorophyll in the ocean, which has a few very high values versus the

background of many low values (Campbell and O'Reilly, 1988). The satellite underestimates the high *in-situ* values due to the averaging effect on the sub-pixel spatial variability. It is therefore important to collect *in-situ* data in regions where the parameter of interest has relatively stable spatial variability (Gordon et al., 1983). However, these discrepancies were more evident for Chl_a measurements than for AOT, where differences were very low and negligible.

Table 3.3 Analysis of variance: Ground-based and Satellite AOT Data

Source	SS	df	MS	F
Treatment	0.002904	1	0.002904	1.06
Block	0.762438	11	0.069313	
Error	0.03011	11	0.002738	
Total	0.79546	23		

α 0.05

Table 3.4 Analysis of variance: *in-situ* and Satellite Chlorophyll Data

Source	SS	df	MS	F
Treatment	0.29108	1	0.29108	26.45
Block	1.584043	24	0.066002	
Error	0.26413	24	0.011006	
Total	2.13926	49		

α 0.05

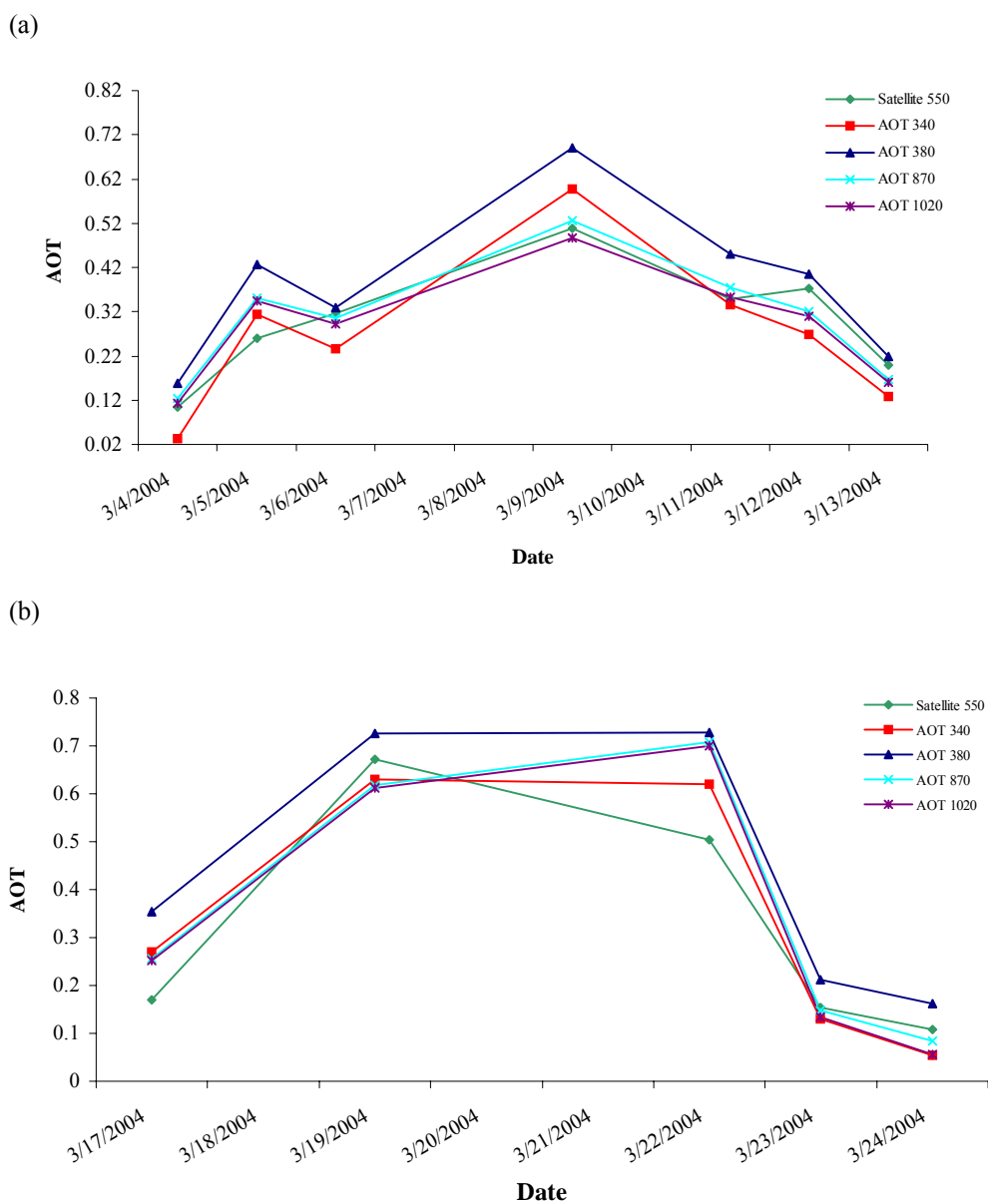


Figure 3.2 Satellite (Giovanni - MODIS Aqua 550) and ground-based aerosol optical thickness during AEROSE 2004 first leg (a) and second leg (b).

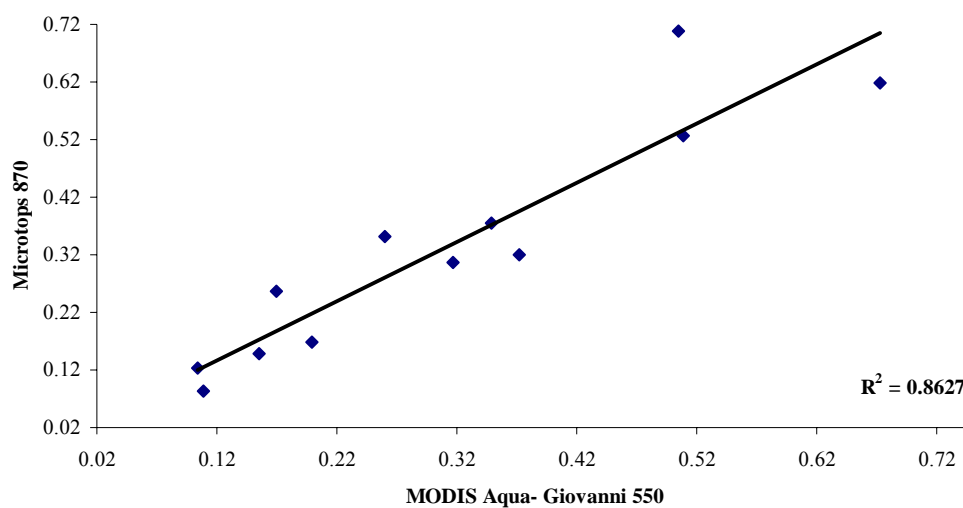


Figure 3.3 Linear relation of daily averaged Giovanni - MODIS Aqua AOT (550) and AEROSOL ground-based AOT (870) during March 2004.

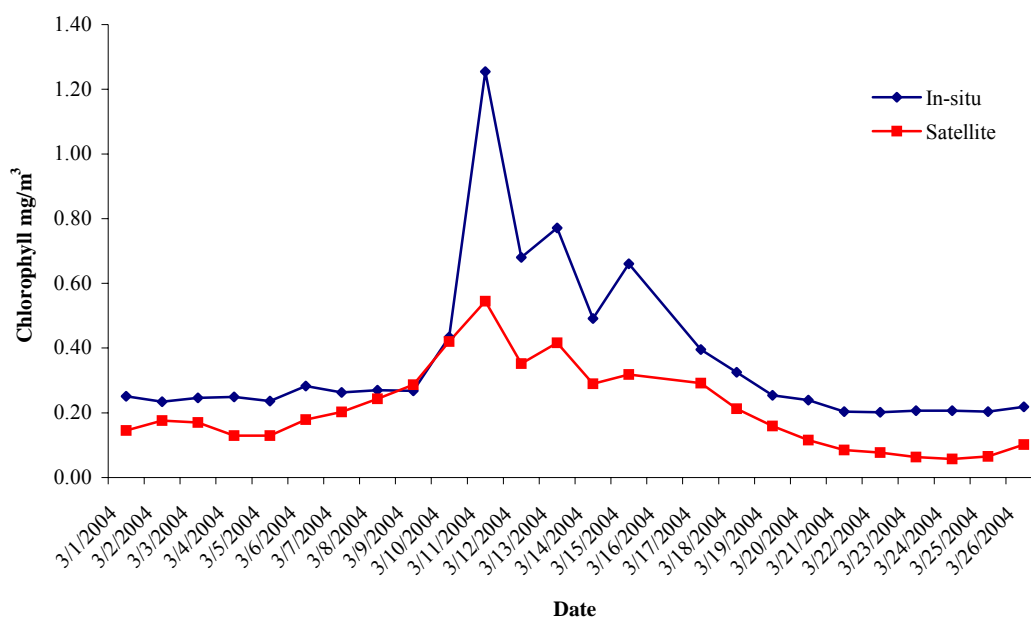


Figure 3.4 Giovanni Assimilated Total Chlorophyll (NOBM) and *in-situ* chlorophyll a concentration (AEROSE 2004).

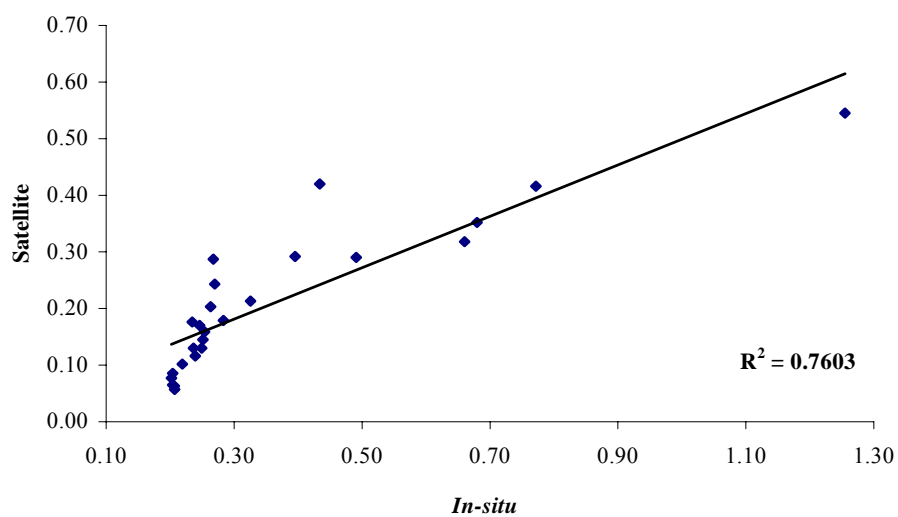


Figure 3.5 Linear relationship of Giovanni Assimilated Total Chlorophyll (NOBM) and *in-situ* chlorophyll concentration (AEROSE 2004).

A time series from August 2002 to December 2005 of monthly Giovanni's AOT and Chl_a products was performed for the Western Atlantic Station (Figure 3.6). Results show that episodes of elevated aerosol dust were followed by an increase in Chl_a concentration approximately one month later. These results confirms our observations from Chapter I, where it was established that a time lag of one month might be necessary for dust to deposit, iron dissolution and iron assimilation by the phytoplankton species present in the region.

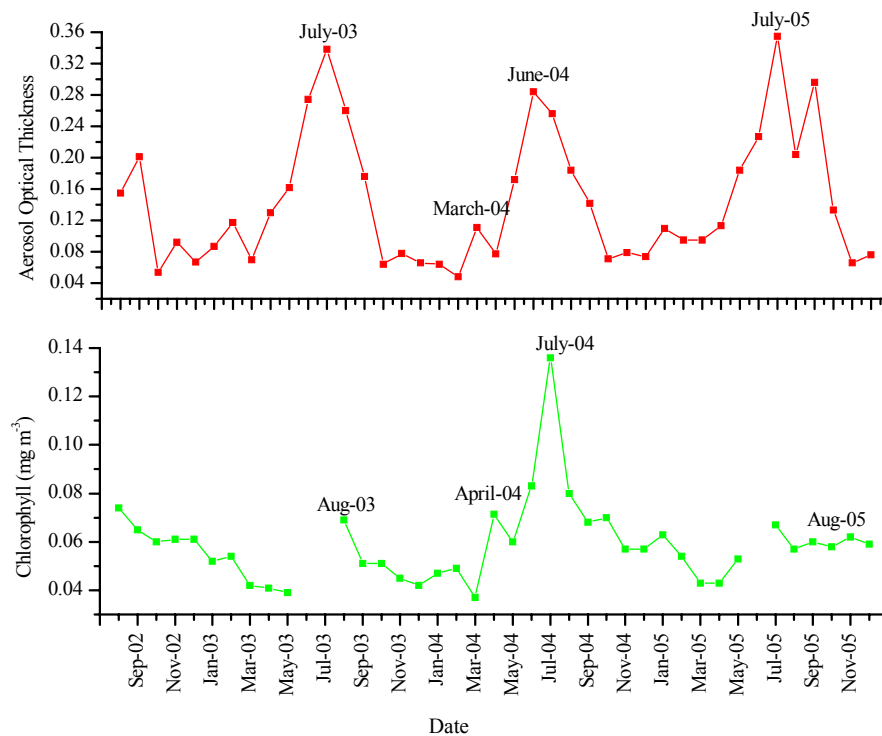


Figure 3.6 Time series (Aug. 2002-Dec. 2005) of monthly averaged Giovanni's AOT (550) and Chl_a for the Western Atlantic Ocean (19 °N, 57 °W).

Giovanni's monthly AOT 550 (MODIS Aqua) was compared with NAO index for 2004 (Figure 3.7) and from 2003–2007 (Figure 3.8). No significant relationship ($R = -0.15$) was observed for the studied area between NAO Index and AOT values (Figure 3.9). Other authors have found low correlations, especially during the summer months. Ginoux et al. (2004) analyzed data from December to March of dust concentrations in Barbados with NAO index and found a correlation coefficient of $r = 0.67$. However, for other seasons they found no significant correlation. Also, studies of TOMS dust optical thickness and NAO index over the period 1979–2000 for Barbados showed that the NAO year-to-year variability exerted a weak influence on summer dust emission and transport, while it appeared to be dominant during the winter (Chiapello et al., 2005). This is due to the fact that the NAO is stronger during winter and its effect on Saharan dust transport is more important during this season (Chiapello and Moulin, 2002). The low correlation found in this study might be related to the fact that the largest African dust intrusion to the studied area occurs mostly during the summer and is minimal during winter. Dust transport across the North Atlantic is affected by the Intertropical Convergence Zone (ITCZ), which causes latitudinal variation in atmospheric transport. During winter the ITCZ shifts toward lower latitudes ($\sim 5^\circ\text{N}$) and dust transport is mostly to the north of South America. Finally, the low correlation may also be the result of other processes affecting dust concentration, such as local meteorological conditions (Ginoux et al., 2004) variation in dust emissions in source region, changes in dust transport paths or removal during transit (Prospero and Lamb, 2003).

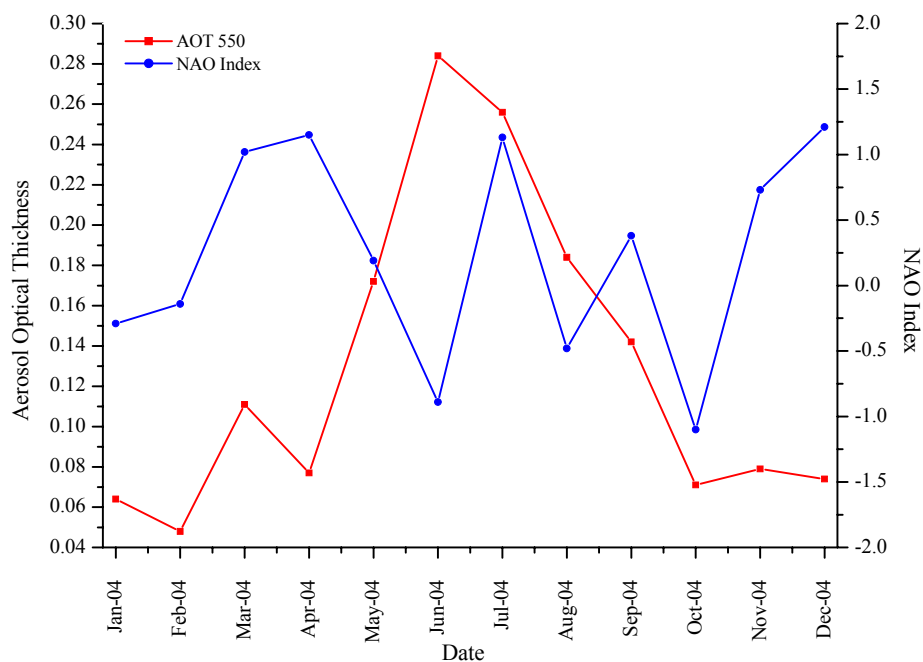


Figure 3.7 Plot of the NAO index and Giovanni's Monthly AOT (550) at Western Atlantic Station (19°N, 57°W) for 2004.

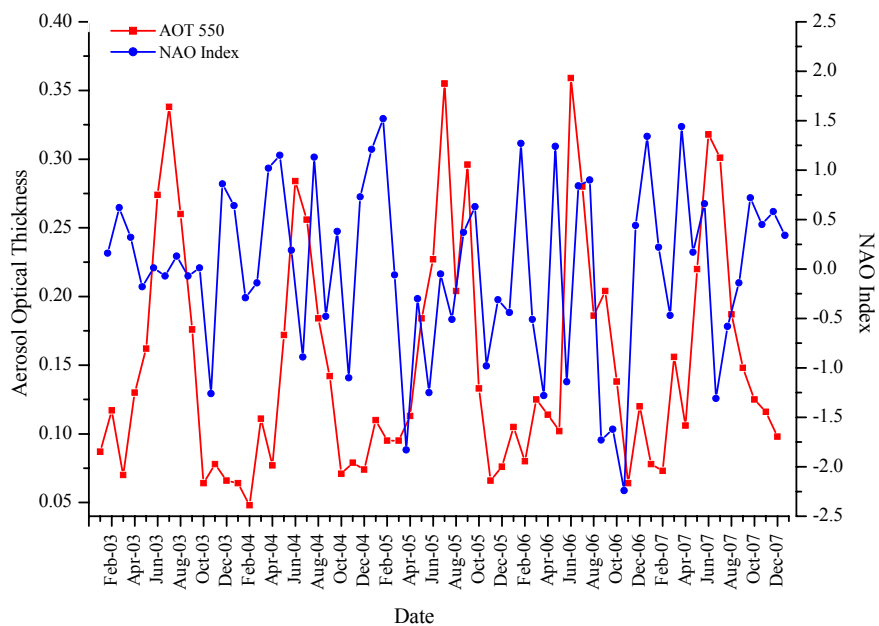


Figure 3.8 Plot of the NAO index and Giovanni's Monthly AOT (550) at Western Atlantic Station (19°N, 57°W) from 2003 to 2007.

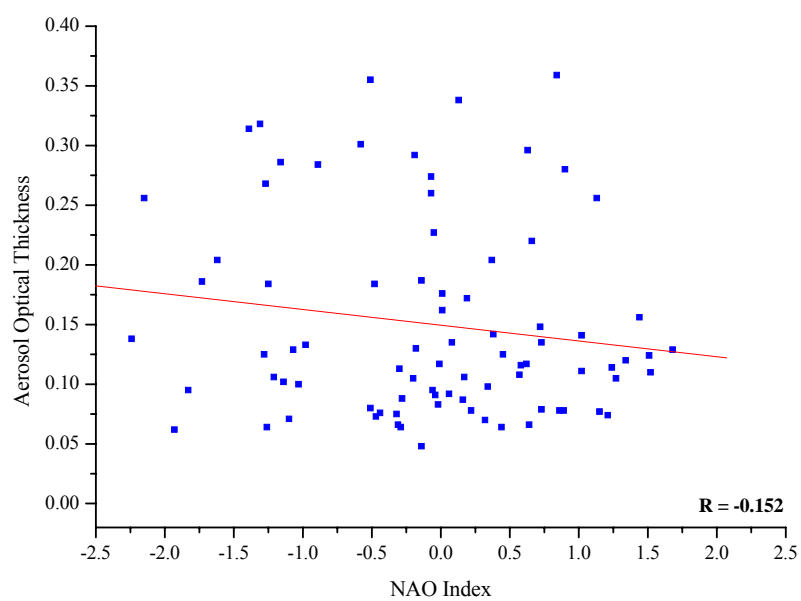


Figure 3.9 Linear relation between the NAO index and Giovanni's monthly AOT (550) data for the Western Atlantic Station (2003 – 2007).

3.4 Conclusions

Shipboard measurements provide high-quality, accurate data but are costly in terms of time and effort and are limited in duration and area of observations. In contrast, satellites can be used to obtain estimates of bio-optical and atmospheric properties over extended spatial and temporal scales, but can be subjected to several sources of error. To fully understand aerosol distribution and their effect on the ocean's biogeochemical cycles requires continuous observations from satellites, ground-based instruments and field experiments. It is necessary to validate satellite data with ground-based observations. This study was intended to observe how well satellite measurements described atmospheric and oceanographic bio-optical properties by comparing AOT and Chl_a satellite and ground-based data. Giovanni (AOT 550, MODIS Aqua) and sun-photometer (Microtops) data were used to assess aerosol optical thickness for the North Atlantic Ocean during March 2004. Atmospheric AOT at 550 nm was compared with Microtops AOT 870 nm; two wavelengths typically used for describing atmospheric dust particles. The results confirm good agreement between satellite and ground-based AOT ($R^2=0.86$), indicating that satellite derived AOT can be validated using sun-photometer observations. This study suggests that MODIS AOT 550 data provide accurate information of the aerosol loading for the North Atlantic Ocean.

Measurements of satellite and *in-situ* Chl_a also showed a strong linear relation ($R^2 = 0.76$). However, an analysis of variance resulted in significant differences between Giovanni's Assimilated Total Chlorophyll product and ground-based measurements due to underestimation of satellite Chl_a throughout the studied area. Satellite underestimation results from the averaging effect of satellite estimates and the distribution of Chl_a in open waters, where a few high values are averaged over a background of many low values.

Therefore, further information of the spatial variability of chlorophyll concentration in the studied area should be taken into consideration when comparing *in-situ* and satellite Chl_a data.

The time series of Giovanni's AOT 550 and Chl_a products presented similar results as those discussed in Chapter I. Peaks in AOT values were followed by an increase in Chl_a concentration nearly one month later. This time lag, also observed in Chapter I, might be the time required for dust deposition, iron dissolution and assimilation by phytoplankton species. This result indicates that a relationship between African dust and Chl_a concentration can be established using Giovanni's satellite products. However, there are some limitations in the use of Giovanni's products for regional observations such as those analyzed on Chapter I. For example, Giovanni has a lower spatial resolution (1°) than MODIS (4km) or SeaWiFS (9km) for AOT and Chl_a ocean products and therefore cannot provide the same detailed information. Also, Giovanni's Chl_a is not produced by direct satellite observations. It is the result of complex calculations generated by the NASA Ocean Biogeochemical Model (NOBM) based on data assimilation of remotely sensed Chl_a.

Finally, no significant correlation was observed between the March 2004 dust event and the North Atlantic Oscillation for our studied area. It has been observed that the NAO has a weak influence on dust emission and transport during the summer (Chiapello et al., 2005) due to the fact that the NAO is much stronger in winter (Chiapello and Moulin, 2002). Since winter months represent the lowest dust input to our studied area, African dust concentrations might have resulted from factors other than the NAO such as local meteorological conditions.

General Conclusions

This study demonstrated a significant relationship between aerosol optical thickness and chlorophyll concentration in the Tropical North Atlantic Ocean using satellite remote sensing data. Saharan dust particles provide iron, a limiting nutrient for phytoplankton's primary production, to the surface waters of the TNAO.

The specific conclusions from this investigation are:

- The TNAO is exposed to an annual fluctuation in AOT that responds to the seasonal variation of Saharan dust storms.
- Annual fluctuations in AOT and Chl_a concentration were observed in CaTS and Western Atlantic stations.
- Satellite imagery showed a connection between aerosol load and phytoplankton biomass.
- A time-lag of one month was observed between AOT and Chl_a maximums at the Western Atlantic Station. This time delay may be associated to deposition, dissolution and assimilation of Fe by phytoplankton.
- Visible reflectance spectroscopy coupled with first derivative analysis is a practical tool to detect iron oxides in desert mineral dust samples.
- ICP-MS element analysis quantified Fe and Al content in our samples.
- As African dust is transported across the Atlantic and the particle size is reduced, the percent of Fe and Al increases. Therefore, these fine particles may supply phytoplankton's Fe requirements at large distances from their geological formation.

- A strong linear relationship ($R=0.93$) was observed between satellite derived AOT and ground-based data.
- Giovanni's satellite Chl_a data was underestimated with respect to *in-situ* measurements.
- The weak NAO observed during the summer months does not have a significant effect over the seasonal patterns of Saharan dust intrusions in the Tropical Western Atlantic region.

Appendix A

Time Series Plots of Aerosol Optical Thickness and Chlorophyll_a Pigment Concentration for the Three Stations Studied:

A. Caribbean Time Series Station (CaTS)

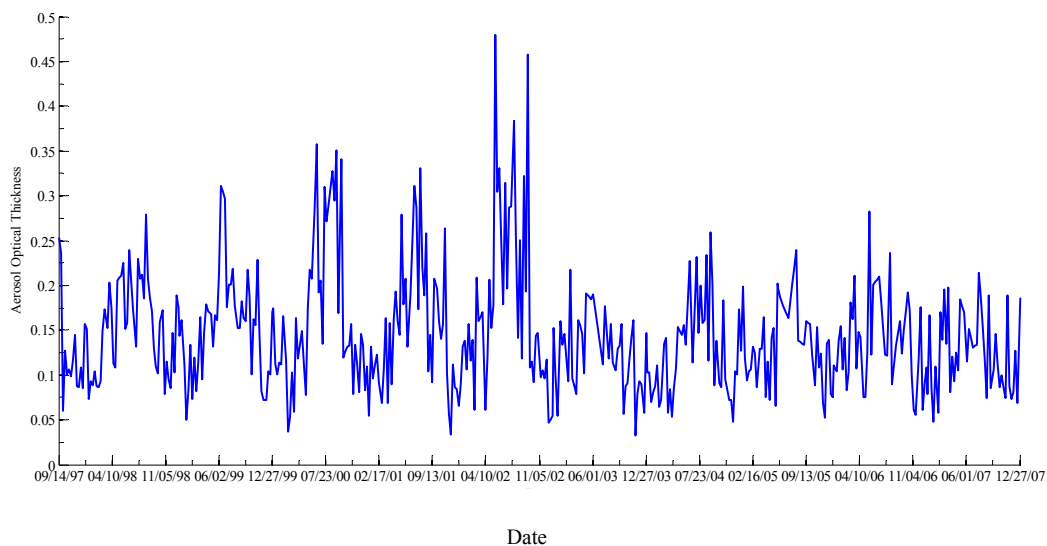


Figure A.1 Time plot of aerosol optical thickness at CaTS (Sept. 1997 – Dec. 2007)

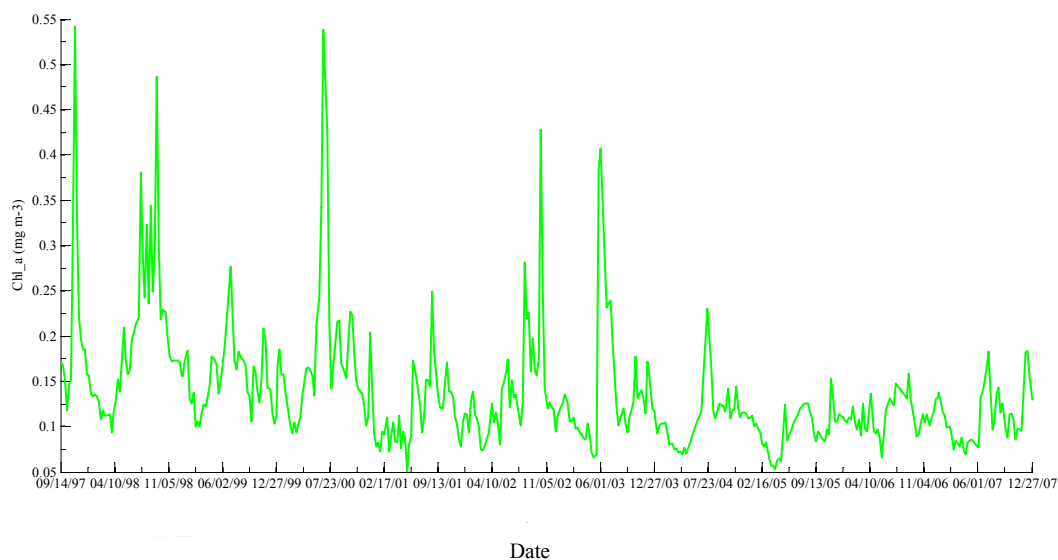


Figure A.2 Time plot of chlorophyll concentration at CaTS (Sept. 1997 – Dec. 2007).

B. Western Atlantic Ocean

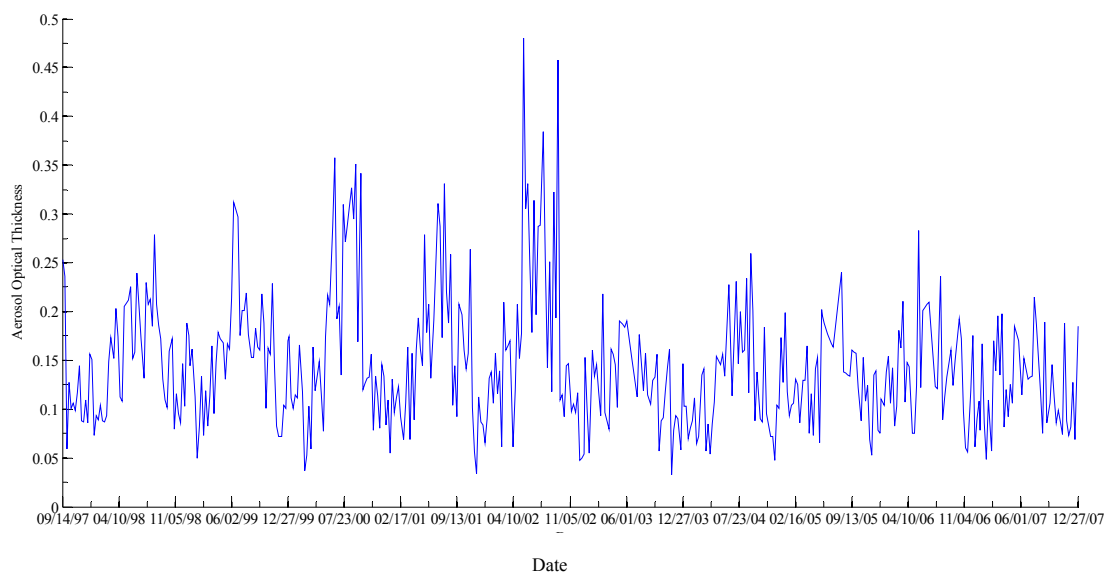


Figure A.3 Time plot of aerosol optical thickness at Western Atlantic Station (Sept. 1997 – Dec. 2007).

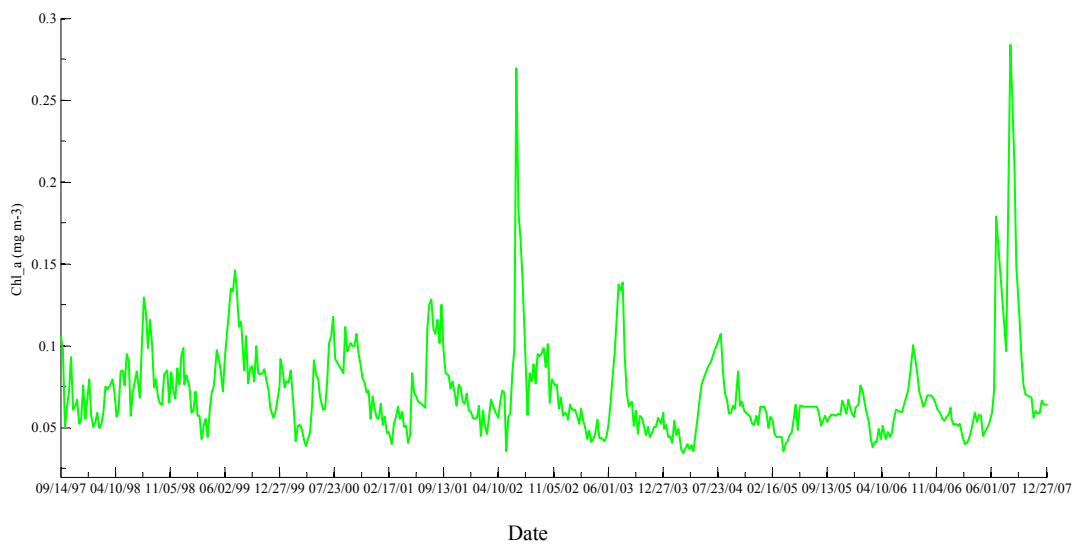


Figure A.4 Time plot of chlorophyll concentration at Western Atlantic Station (Sept. 1997 – Dec. 2007).

C. Atlantic, North of PR Station

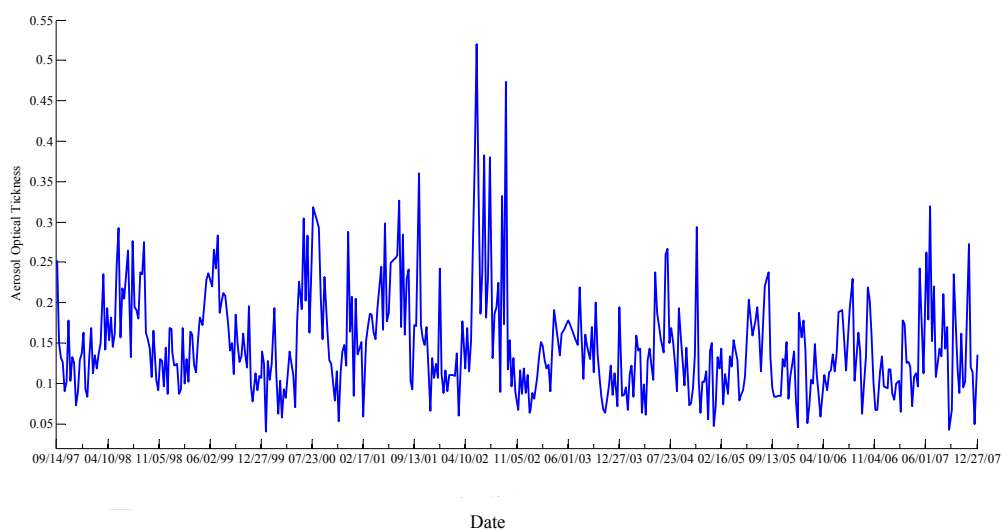


Figure A.7 Time plot of aerosol optical thickness at Atlantic, North of PR Station (Sept. 1997 – Dec. 2007).

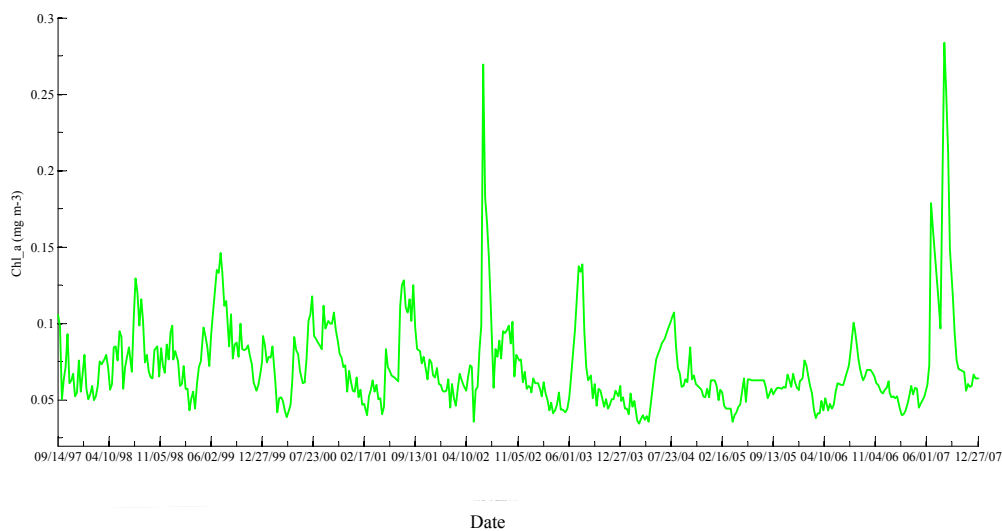


Figure A.8 Time plot of chlorophyll concentration at Atlantic, North of PR Station (Sept. 1997 – Dec. 2007).

Literature Cited

- Aloysius, M., Mohan, M., Suresh Babu, S., Parameswaran, K. and Moorthy, K. K. 2009. Validation of MODIS derived aerosol optical depth and an investigation on aerosol transport over the South East Arabian Sea during ARMEX-II. *Annales Geophysicae*, 27, 2285–2296.
- Arimoto, R., Balsam, W., and Schloesslin, C. 2002. Visible spectroscopy of aerosol particles collected on filters: iron-oxide minerals. *Atmospheric Environment*, 36, 89-96.
- Baker, A. R. and Jickells, T. D. 2006. Mineral particle size as a control on aerosol iron solubility. *Geophysical Research Letters*, 33, L17608, 1-4.
- Baker, A.R., Jickells, T.D., Witt, M. and Linge, K.L. 2006. Trends in the solubility of iron, aluminium, manganese and phosphorus in aerosol collected over the Atlantic Ocean. *Marine Chemistry*, 98, 43-58.
- Bates, T. S., Quinn, P. K., Coffman, D. J., Johnson, J. E., Miller, T. L., Covert, D. S., Wiedensohler, A., Leinert, S., Nowak, A. and Neusüss, C. 2001. Regional physical and chemical properties of the marine boundary layer aerosol across the Atlantic during Aerosols99: An overview. *Journal Geophysical Research*, 106, 20, 767–782.
- Bonnet, S. and Guieu, C. 2004. Dissolution of atmospheric iron in seawater. *Geophysical Research Letters*, 31, 1-4.
- Bonnet, S., Guieu, C., Chiaverini, J., Ras, J. and Stock, A. 2005. Effect of atmospheric nutrients on the autotrophic communities in low nutrient low chlorophyll system. *Limnology and Oceanography*, 50 (6), 1810-1819.
- Brown, D. J., Shepherd, K. D., Walsh, M. G., Mays, M. D. and Reinsch, T. G. 2006. Global soil characterization with VNIR diffuse reflectance spectroscopy. *Geoderma*, 132, 273–290.
- Campbell, J.W. and O'Reilly, J.E. 1988. Role of satellites in estimating primary productivity on the northwest Atlantic continental shelf. *Continental Shelf Research*, 8, 179–204.
- Campbell, J.W. 2005. The MODIS Chlorophyll a Product: Strategy and Recommendations. MODIS Science Team Meeting Baltimore, MD March 22-24, 2005.
http://modis.gsfc.nasa.gov/sci_team/meetings/200503/presentations/ocean/campbell.pdf
- Capone, D.G., Burns, J.A., Montoya, J.P., Subramaniam, A., Mahaffey, C., Gunderson, T., Michaels, A.F. and Carpenter, E.J. 2005. Nitrogen fixation by *Trichodesmium spp.*: An important source of new nitrogen to the tropical and subtropical North Atlantic Ocean. *Global Biogeochemical Cycles*, 19, 1-17.
- Carpenter, E.J. and Romand, K. 1991. Major Role of the Cyanobacterium *Trichodesmium* in Nutrient Cycling in the North Atlantic Ocean. *Science*, 254 (5036), 1356 – 1358.

Castillo, S., Moreno, T., Querol, X., Alastuey, A., Cuevas E., Herrmann, L., Mounkaila, M., and Gibbons, W. 2008. Trace element variation in size-fractionated African desert dusts. *Journal of Arid Environments*, 72, 1034–1045.

Chiapello, I. and Moulin, C. 2002. TOMS and METEOSAT satellite records of the variability of Saharan dust transport over the Atlantic during the last two decades (1979-1997). *Geophysical Research Letters*, 29 (8), 1176.

Chiapello, I., Moulin, C. and Prospero, J. M. 2005. Understanding the long-term variability of African dust transport across the Atlantic as recorded in both Barbados surface concentrations and large-scale Total Ozone Mapping Spectrometer (TOMS) optical thickness. *Journal of Geophysical Research*, 110, D18S10, 1-9.

Chuanmin H., Montgomery, E.T., Schmitt, R.W. and Muller-Karger, F.E. 2004. The dispersal of the Amazon and Orinoco River water in the tropical Atlantic and Caribbean Sea: Observation from space and S-PALACE floats. *Deep-Sea Research II*, 51, 1151–1171.

Claustre, H., Morel, A., Hooker, S.B., Babin, M., Antoine, D., Oubelkheir, K., Bricaud, A., Leblanc, K., Quéguiner, B. and Maritorena, S. 2002. Is desert dust making oligotrophic waters greener? *Geophysical Research Letters*, 29 (10), 107-1 – 107-4.

Cullen, J.J. and Neale, P.J. 1994. Ultraviolet radiation, ozone depletion, and marine photosynthesis. *Photosynthesis Research*, 39, 303-320.

Deaton, B.C. and Balsam, W.L. 1991. Visible spectroscopy- a rapid method for determining hematite and goethite concentration in geological materials. *Journal of Sedimentary Petrology*, 6, 628–632.

Del Castillo, C.E.D., Coble, P.G., Morell, J.M., Lopez, J.M. and Corredor, J.E. 1999. Analysis of the optical properties of the Orinoco River plume by absorption and fluorescence spectroscopy. *Marine Chemistry*, 66, 35–51.

Darecki, M. and Stramski, D. 2004. An evaluation of MODIS and SeaWiFS bio-optical algorithms in the Baltic Sea. *Remote Sensing of Environment*, 89, 326–350.

Duce, R. A., and Tindale, N. M. 1991. Atmospheric transport of iron and its deposition in the ocean. *Limnology and Oceanography*, 36, 1715-1726.

Elias, M., Chartier, C., Prévo, G., Garay, H. and Vignaud, V. 2006. The colour of ochres explained by their composition. *Materials Science and Engineering*, B-127, 70–80.

Esaias, W.E., Abbott, M.R., Barton, I., Brown, O.B., Campbell, J.W., Carder, K.L., Clark, D.K., Evans, R.H., Hoge, F.E., Gordon, H.R., Balch, W.M., Letelier, R., and Minnett, P.J. 1998. An Overview of MODIS Capabilities for Ocean Science Observations. *Transactions on Geosciences and Remote Sensing*, 36 (4), 1250-1256.

Falciani, R., Novaro, E., Marchesini, M. and Gucciardi, M. 2000. Multi-element analysis of soil and sediment by ICP-MS after a microwave assisted digestion method. *J. Anal. At. Spectrom.*, 15, 561-565.

Fan Song-Miao., Moxim, W.J. and Levy II, H. 2006. Aeolian input of bioavailable iron to the ocean. *Geophysical Research Letters*, 33, L07602, 1-4.

Gao, B.C., Montes, M.J., Li, R.R., Dierssen, H.M. and Davis, C.O. 2007. An atmospheric correction algorithm for remote sensing of bright coastal waters using MODIS land and ocean channels in the solar spectral region. *IEEE Transactions on Geoscience and Remote Sensing*, 45(6), 1835-1843.

Gargett, A. and Marra, J. 2002. *The Sea: Biological-Physical Interactions in the Sea. Effects of Upper Ocean Physical Processes (Turbulence, Advection and Air–Sea Interaction) On Oceanic Primary Production.* Chapter 2, 12, 19-44.

Gilbes, F., Armstrong, R.A., Webb, R.M.T. and Müller-Karger, F.E. 2001. SeaWiFS Helps Assess Hurricane Impact on Phytoplankton in Caribbean Sea. *Eos, Transactions, American Geophysical Union*, 82 (45), 529-533.

Gilbes, F. and Armstrong, R. 2004. Phytoplankton dynamics in the eastern Caribbean Sea as detected with space remote sensing. *Int. J. Remote Sensing*, 10–20 (25), 1449–1452.

Ginoux, P., Prospero, J.M, Torres, O. and Chin, M. 2004. Long-term simulation of global dust distribution with the GOCART model: correlation with North Atlantic Oscillation. *Environmental Modelling & Software*, 19, 113–128.

González, N. M., Müller-Karger, F. E., Cerdeira Estrada, S., Pérez de los Reyes, R., Victoria del Río, I., Cárdenas Pérez, P. and Mitrani Arenal, I. 2000. Near-surface phytoplankton distribution in the western intra-Americas seas: The influence of El Niño and weather events. *Journal of Geophysical Research*, 105 (C6), 14,029 –14,043.

Gordon, H. R., Clark, D. K., Brown, J. W., Brown, O. B., Evans, R. H. and Broenkow, W. W. 1983. Phytoplankton pigment concentrations in the Middle Atlantic Bight: Comparison of ship determinations and CZCS estimates. *Applied Optics*, 22 (1), 20–36.

Gordon, H. R. and Wang, M. 1994. Retrieval of water leaving radiance and aerosol optical thickness over the oceans with SeaWiFS: A preliminary algorithm. *Applied Optics*, 33 (3), 443–452.

Goudie, A.S. and Middleton, N.J. 2001. Saharan dust storms: nature and consequences. *Earth-Science Reviews*, 56, 179–204.

Gregg, W.W. and Conkright, M.E. 2001. Global seasonal climatologies of ocean chlorophyll: Blending in situ and satellite data for the Coastal Zone Color Scanner era. *Journal of Geophysical Research*, 106 (C2), 2499–2515.

Gregg, W.W. 2002. A Coupled Ocean-Atmosphere Radiative Model for Global Ocean Biogeochemical Models. NASA GSFC Technical Report Series on Global Modeling and Data Assimilation, 104606, 22.

Gregg, W.W. 2008. Assimilation of SeaWiFS ocean chlorophyll data into a three-dimensional global ocean model. *Journal of Marine Systems*, 69, 205–225.

Guieu, C., Loye-Pilot, M.D., Ridame, C. and Thomas, C. 2002. Chemical characterization of the Saharan dust end-member: Some biogeochemical implications for the western Mediterranean Sea. *Journal of Geophysical Research*, 107 (D15), 5-1 – 5-11.

Holm-Hansen, O., Kahru, M., Hewes, C.D., Kawaguchi, S., Kameda, T., Sushin, V.A., Krasovski, I., Priddle, J., Korb, R., Hewitt, R.P. and Mitchell, B.G. 2004. Temporal and spatial distribution of chlorophyll- a in surface waters of the Scotia Sea as determined by both shipboard measurements and satellite data. *Deep-Sea Research II*, 5, 1323–1331.

Huete, A. R. and Escadafal, R. 1991. Assessment of Biophysical Soil Properties Through Spectral Decomposition Techniques. *Remote Sensing of the Environment*, 35, 149-159.

Hurrell, J.W. 1995. Decadal trend in the North Atlantic Oscillation: regional temperatures and precipitations. *Science*, 269, 676–679.

Jickells, T. D., An, Z. S., Andersen, K. K., Baker, A. R., Bergametti, G., Brooks, N., Cao, J. J., Boyd, P. W., Duce, R. A., Hunter, K. A., Kawahata, H., Kubilay, N., la Roche, J., Liss, P. S., Mahowald, N., Prospero, J. M., Ridgwell, A. J., Tegen, I. and Torres, R. 2005. Global Iron Connections Between Desert Dust, Ocean Biogeochemistry, and Climate. *Science*, 308, 67-71.

Jiménez-Vélez, B., Detrés, Y., Armstrong, R.A. and Gioda, A. 2009 Characterization of African Dust (PM_{2.5}) across the Atlantic Ocean during AEROSE 2004. *Atmospheric Environment*, 43, 2659–2664.

Jokiel, P. L. and York, R. H. 1994 Importance of ultraviolet radiation in Photoinhibition of microalgal growth. *Limnology and Oceanography*, 29 (1), 192-199.

Kaskaoutisa, D.G., Kambezidis, H.D., Nastosb, P.T. and Kosmopoulos, P.G. 2008. Study on an intense dust storm over Greece. *Atmospheric Environment*, 42 (29), 6884-6896.

Kaufman Y.J., Tanré, D. and Boucher, O. 2002. A satellite view of aerosols in the climate system. *Nature*, 419, 215-223

Kaufman, Y. J., Koren, I., Remer, L. A., Tanré, D., Ginoux, P. and Fan, S. 2005. Dust transport and deposition observed from the Terra-Moderate Resolution Imaging Spectroradiometer (MODIS) spacecraft over the Atlantic Ocean. *Journal of Geophysical Research*, 110, 1-16.

Kosmas, C. S., Franzmeier, D. P., and Schulze, D. G. 1986. Relationship among Derivative Spectroscopy, Color, Crystallite Dimensions, and Al Substitution of Synthetic Goethites and Hematites. *Clays and Clay Minerals*, 34 (6), 625-634.

Kustka, A., Carpenter, E.J. and Sañudo-Wilhelmy, S.A. 2002. Iron and marine nitrogen fixation: progress and future directions. *Research in Microbiology*, 153, 255–262.

Lavendera, S.J., Pinkerton, M.H., Moored, G.F., Aikend, J. and Blondeau-Patissier, D. 2005. Modification to the atmospheric correction of SeaWiFS ocean colour images over turbid waters. *Continental Shelf Research*, 25, 539–555.

Lenes, J.M., Darrow, B.P., Catrall, C., Heil, C.A., Callahan, M., Vargo, G.A., Byrne, R.H., Prospero, J.M., Bates, D.E., Fanning, K.A. and Walsh, J.J. 2001. Iron fertilization and the *Trichodesmium* response on the West Florida shelf. *Limnology Oceanography*, 46 (6), 1261–1277.

Mahowald, N. M., Baker, A. R., Bergametti, G., Brooks, N., Duce, R. A., Jickells, T. D., Kubilay, N., Prospero, J. M., and Tegen, I. 2005. Atmospheric global dust cycle and iron inputs to the ocean, *Global Biogeochemical Cycles*, 19, GB4025, 1-15.

Mallet, M., Chami, M. Gentili, B. Sempéré, R. and Dubuisson, P. 2009. Impact of sea-surface dust radiative forcing on the oceanic primary production: A 1D modeling approach applied to the West African coastal waters. *Geophysical Research Letters*, 36, L15828.

Martin, J.H., Gordon, R.M. and Fitzwater, S.E. 1991. The case for iron. *Limnology and Oceanography*, 36, 1793-1802.

Martin, J. H., Coale, K. H., Johnson, K. S., Fitzwater, S. E., Gordon, R. M., Tanner, S. J., Hunter, C. N., Elrod, V. A., Nowicki, J. L., Coley, T. L., Barber, R. T., Lindley, S., Watson, A. J., Van Scoy, K., Law, C. S., Liddicoat, M. I., Ling, R., Stanton, T., Stockel, J., Collins, C., Anderson, A., Bidigare, R., Ondrusek, M., Latasa, M., Millero, F. J., Lee, K., Yao, W., Zhang, J. Z., Friederich, G., Sakamoto, C., Chavez, F., Buck, K., Kolber, Z., Greene, R., Falkowski, P., Chisholm, S. W., Hoge, F., Swift, R. and Yungel, J. 1994. Testing the iron hypothesis in ecosystems of the equatorial Pacific Ocean. *Nature*, 371, 123–129.

Mills, M.M., Ridame, D.M., La Roche, J. and Geider, R.J. 2004. Iron and phosphorus co-limit nitrogen fixation in the eastern tropical North Atlantic. *Nature*, 429, 292-294.

Moore, K.J., Abbott, M.R., Richman, J.G., Smith, W.O., Cowles, T.J., Coale, K.H., Gardner, W.D., and Barber, R.T. 1999. SeaWiFS satellite ocean color data from the Southern Ocean, *Geophysical Research Letter*, 26 (10), 1465–1468.

Moore, K.J., Doney, S.C., Lindsay, K., Mahowald, N. and Michael, A.F. 2006. Nitrogen fixation amplifies the ocean biogeochemical response to decadal timescale variations in mineral dust deposition. *Tellus*, 58B, 560–572.

Moore, M.C., Mills, M.M., Milne, A., Langlois, R., Achterberg, E.P., Lochte, K., Geider, R.J. and La Roche, J. 2006. Iron limits primary productivity during spring bloom development in the central North Atlantic. *Global Change Biology*, 12 (4), 626 – 634.

Moore, C.M., Mills, M.M., Achterberg, E.P., Geider, R.J., LaRoche, J., Lucas, M.I., McDonagh, E.L., Pan, X., Poulton, A.J., Rijkenberg, M.J.A., Suggett, D.J., Ussher, S.J. and Woodward, E.M.S. 2009. Large-scale distribution of Atlantic nitrogen fixation controlled by iron supply. *Nature Geoscience*, 2, 867-871.

Moreno, T., Querol, X., Castillo, S., Alastuey, A., Cuevas, E., Herrmann, L., Mounkaila, M., Elvira, J. and Gibbons, W. 2006. Geochemical variations in aeolian mineral particles from the Sahara–Sahel Dust Corridor. *Chemosphere*, 65, 261–270

Morris, V., Clemente-Colón, P., Nalli, N.R., Joseph, E., Armstrong, R.A., Detrés, Y., Goldberg, M.D., Minnett, P.J. and Lumpkin, R. 2006. Measuring Trans-Atlantic Aerosol Transport from Africa. *Eos*, 87 (50), 565-580.

Moulin, C., Lambert, C. E., Dulac, F. and Dayan, U. 1997. Control of atmospheric export of dust from North Africa by the North Atlantic Oscillation. *Nature*, 387, 691-694.

Müller-Karger, F.E., McClain, C.R. and Richardson, P.L. 1988. The dispersal of the Amazon's water. *Nature*, 333, 56–58.

Müller-Karger, F.E., McClain, C.R., Fisher, T.R., Esaias, W.E. and Varela, R. 1989. Pigment distribution in the Caribbean Sea: Observations from space. *Prog. Oceanog.*, 23, 23 - 64.

Myhre, G., et al. 2005. Intercomparison of satellite retrieved aerosol optical depth over ocean during the period September 1997 to December 2000. *Atmos. Chem. Phys.*, 5, 1697–1719.

O'Reilly, J.E., Maritorena, S., Mitchell, B.G., Siegel, D.A., Carder, K.L., Garver, S.A., Kahru, M. and McClain C. 1998. Ocean color chlorophyll algorithms for SeaWiFS. *Journal of Geophysical Research*, 103 (24), 937–953.

O'Reilly, J.E. et al. 2000. SeaWiFS Post-launch Calibration and Validation Analyses, Part 3. SeaWiFS Post-launch Technical Report Series. NASA/TM-2000-206892, NASA Goddard Space Flight Center, 11, 50.

O'Reilly, J.E. 2000. Will SeaWiFS and MODIS/Aqua products be different if $L_w(\lambda)$ is perfectly retrieved? http://oceancolor.gsfc.nasa.gov/DOCS/seawifs_modis_diff.pdf.

Piketh, S.J., Tyson, P.D. and Steffen, W. 2000. Aeolian transport from southern Africa and iron fertilization of marine biota in the south Indian Ocean. *South African Journal of Science*, 96 (5), 244 - 246.

Prospero, J.M. and Carlson, T.B. 1972. Vertical and areal distribution of Saharan dust over the Western Equatorial North Atlantic Ocean. *Journal of Geophysical Research*, 77 (27), 5255-5265.

Prospero, J.M., Glaccum, R.A. and Nees, R.T. 1981. Atmospheric transport of soil dust from Africa to South America. *Nature*, 289, 570–572.

Prospero, J.M., Olmez, I. and Ames, M. 2001. Al and Fe in PM_{2.5} and PM₁₀ suspended particles in South Central Florida: the impact of the long range transport of African mineral dust. *J. Water Air Soil Poll.*, 125, 291-317.

Prospero, J.M., Ginoux, P., Torres, O., Nicholson, S.E. and Gill, T.E. 2002. Environmental Characterization of Global Sources of Atmospheric Soil Dust Identified with the Nimbus 7 Total Ozone Mapping Spectrometer (TOMS) Absorbing Aerosol Product. *Reviews of Geophysics*, 40 (1), 2-1 – 2-31.

Prospero, J.M. and Lamb, P.J. 2003. African droughts and dust transport to the Caribbean: climate change implications. *Science*, 302, 1024-1027.

Prospero, J.M. and Landing, W. 2009. African dust deposition to Florida: How well do dust models perform? *IOP Conf. Ser.: Earth Environmental Science*, 7, 012-015.

Remer, L. A., Kaufman, Y. J. et al. 2005. The MODIS aerosol algorithm, products, and validation. *Journal of the Atmospheric Sciences*, 62 (4), 947-973.

Retalis A. and Hadjimitsis, D. G., 2010. Comparison of aerosol optical thickness with in situ visibility data over Cyprus. *Nat. Hazards Earth Syst. Sci.*, 10, 421–428.

Robinson, A. R., McCarthy, J. J. and Rothschild, B. J. 2002. The Sea: Biological-Physical Interactions in the Sea. Introduction- Biological-Physical Interactions in the Sea: Emergent Findings and New Directions. Chapter 1, 12, 1-17.

Sarthou, G., Baker, A.R., Blain, S., Achterberg, E.P., Boye, M., Bowie, A.R., Croot, P., Laan, P., de Baar, H.J.W., Jickells, T.D. and Worsfol, P.J. 2003. Atmospheric iron deposition and sea-surface dissolved iron concentrations in the eastern Atlantic Ocean. *Deep-Sea Research I*, 50, 1339–1352.

di Sarra, A., Cacciani, M. Chamard, P., Cornwall, C., DeLuisi, J.J., Di Iorio, T., Disterhoft, P., Fiocco, G., Fuà, D. and Monteleone, F. 2002. Effects of desert dust and ozone on the ultraviolet irradiance at the Mediterranean island of Lampedusa during PAUR II. *Journal of Geophysical Research*, 107 (D18), 8135.

Savtchenko, A., Ouzounov, D., Ahmad, S., Acker, J., Leptoukh, G., Koziana, J. and Nickless, D. 2004. Terra and Aqua MODIS products available from NASA GES DAAC. *Advances in Space Research*, 34, 710–714.

Scheinos, A. C., Chavernas, A., Barron, V. and Torrent, J. 1998. Use and limitations of second-derivative diffuse reflectance spectroscopy in the visible to near-infrared range to identify and quantify Fe oxide minerals in soils. *Clays and Clay Minerals*, 46 (5), 528-536.

Scheinos, A. C and Schwertmann, U. 1999. Color Identification of Iron Oxides and Hydrosulfates: Use and Limitations. *Soil Sci. Soc. Am. J.*, 63, 1463-1471.

Schopf, P. and Lough, A. 1995. A reduced-gravity isopycnic ocean model-hindcasts of El-Niño. *Mon. Weather Rev.*, 123, 2839-2863.

Shen S., Rui, H., Liu, Z., Zhu, T. Lu, L., Berrick, S., Leptoukh, G., Teng, W., Acker, J., Johnson, J., Ahmad, S. P., Savtchenko, A., Gerasimov, I. and Kempler, S. Giovanni: A System for Rapid Access, Visualization and Analysis of Earth Science Data Online. (<http://giovanni.gsfc.nasa.gov>).

Shen, Z.X., Cao, J.J., Zhang, X.Y., Arimoto, R., Ji, J.F., Balsam, W.L., Wang, Y.Q., Zhang, R.J. and Li, X.X. 2006. Spectroscopic analysis of iron-oxide minerals in aerosol particles from northern China. *Science of the Total Environment*, 367, 899-907.

Stegman, P.M. 2000. Ocean color satellite and phytoplankton dust connection. *Satellite, Oceanography and Society*, 11, 207-223.

Tanré, D., Kaufman, Y.J, Herman, M. and Mattoo, S. 1997 Remote sensing of aerosol properties over oceans using the MODIS/EOS spectral radiances. *Journal of geophysical research*, 102 (D14), 16971-16988.

The Ring Group 1981. Gulf Stream cold-core rings: their physics, chemistry and biology. *Science*, 212, 1091-1100.

Torrent, J. and Barron, V. 2003. The Visible Diffuse Reflectance Spectrum in Relation to the Color and Crystal Properties of Hematite. *Clays and Clay Minerals*, 51 (3), 309-317.

Ussher, S.J. and Woodward, E.M.S. 2009. Large-scale distribution of Atlantic nitrogen fixation controlled by iron supply. In: *Nature Geoscience*, 2, 867-871.

Wang, J. and Sundar, C.A. 2003. Intercomparison between satellite-derived aerosol optical thickness and PM_{2.5} mass: Implications for air quality studies. *Geophysical Research Letters*, 30 (21), 2095, 4-1 – 4-4.

Wang, M., Bailey, S., McClain, C. R., Pietras, C., and Riley, T. 1999. Remote Sensing of the Aerosol Optical Thickness from SeaWiFS in Comparison with the in situ Measurements. Alps 99 Symposium, Meribel, France, January 18-22, 1999.

Wang, M. 2000. The SeaWiFS atmospheric correction algorithm updates, In: McClain, C.R., Ainsworth, E.J. Barnes, R.A. Eplee, R.E., Patt, F.S. Robinson, W.D. Wang, M. and Bailey,

S.W. SeaWiFS Post-launch Calibration and Validation Analyses, Part 1. NASA Tech. Memo. 2000-206892, Vol. 9, S.B. Hooker and E.R. Firestone, Eds., NASA Goddard Space Flight Center, Greenbelt, Maryland, 57-63.

Warne, A.G., Webb, R.M.T., and Larsen, M.C. 2005. Water, Sediment, and Nutrient Discharge Characteristics of Rivers in Puerto Rico, and their Potential Influence on Coral Reefs: U.S. Geological Survey Scientific Investigations Report 2005-5206, 58.

White, S. N., Sholkovitz, E. R. and Farr, N. 2006. Visible reflectance spectroscopy on a buoy-mounted aerosol sampler: development of a sensor for quantifying the deposition of mineral dust to the oceans, IEEE/MTS Oceans 2006, IEEE Press, Boston, MA.

Wu, J., and Luther III. G.W. 1994. Size-fractionated iron concentrations in the water column of the western North Atlantic Ocean. *Limnology and Oceanography*, 39 (5), 1119-1129.

Wu, J., and Boyle, E. 2002. Iron in the Sargasso Sea: Implications for the processes controlling dissolved Fe distribution in the ocean. *Global Biogeochemical Cycles*, 16 (4), 1086, 33, 1- 8.

Yamazaki, H., Mackas, D. L. and Denman, K. L. 2002. The Sea, Biological-Physical Interactions in the Sea. *Coupling Small-Scale Physical Processes with Biology*. Chapter 3, 12, 51-103.